HHS Public Access

Author manuscript

Free Radic Biol Med. Author manuscript; available in PMC 2017 July 01.

Published in final edited form as:

Free Radic Biol Med. 2016 July ; 96: 99–115. doi:10.1016/j.freeradbiomed.2016.04.009.

Peroxiredoxin 6 (Prdx6) supports NADPH oxidase1 (Nox1)-based superoxide generation and cell migration

Jaeyul Kwon[#a,b], **Aibing Wang**[#c], **Devin J. Burke**[a], **Howard E. Boudreau**[a], **Kristen J. Lekstrom**[a], **Agnieszka Korzeniowska**[a], **Ryuichi Sugamata**[a], **Yong-Soo Kim**[d], **Liang Yi**[c], **Ilker Ersoy**[e], **Stefan Jaeger**[f], **Kannappan Palaniappan**[g], **Daniel R. Ambruso**[h], **Sharon H. Jackson**[c], and **Thomas L. Leto**[a,i]

[a] Laboratory of Host Defenses, National Institute of Allergy and Infectious Diseases, National Institutes of Health, Rockville, MD, USA

[b] Department of Medical Education, School of Medicine, Chungnam National University, Daejeon, 301-747, Korea

[c]Diabetes Cluster, National Institute on Minority Health and Health Disparities, National Institutes of Health, Bethesda, MD, USA

[d] Laboratory of Immunogenetics, National Institute of Allergy and Infectious Diseases, National Institutes of Health, Rockville, MD, USA

[e] Department of Pathology and Anatomical Sciences, University of Missouri, Sch. of Medicine, Columbia, MO, USA

[f] Lister Hill National Center for Biomedical Communications, National Library of Medicine, National Institutes of Health, Bethesda, MD, USA

[g] Department of Computer Sciences, University of Missouri-Columbia, MO, USA

[h] Department of Pediatrics, University of Colorado Sch. of Medicine, Denver, CO, USA

[#] These authors contributed equally to this work.

Abstract

Nox1 is an abundant source of reactive oxygen species (ROS) in colon epithelium recently shown to function in wound healing and epithelial homeostasis. We identified Peroxiredoxin 6 (Prdx6) as a novel binding partner of Nox activator 1 (Noxa1) in yeast two-hybrid screening experiments using the Noxa1 SH3 domain as bait. Prdx6 is a unique member of the Prdx antioxidant enzyme family exhibiting both glutathione peroxidase and phospholipase A_2 activities. We confirmed this interaction in cells overexpressing both proteins, showing Prdx6 binds to and stabilizes wild type

[i] Corresponding author: Laboratory of Host Defenses, NIAID, NIH, 12441 Parklawn Drive, Rockville, MD, 20852, USA. Fax: 301 480-1731. tleto@nih.gov.

Disclosure

The authors declare no conflict of interest.

Noxa1, but not the SH3 domain mutant form, Noxa1 W436R. We demonstrated in several cell models that Prdx6 knockdown suppresses Nox1 activity, whereas enhanced Prdx6 expression supports higher Nox1-derived superoxide production. Both peroxidase- and lipase-deficient mutant forms of Prdx6 (Prdx6 C47S and S32A, respectively) failed to bind to or stabilize Nox1 components or support Nox1-mediated superoxide generation. Furthermore, the transition-state substrate analogue inhibitor of Prdx6 phospholipase A_2 activity (MJ-33) was shown to suppress Nox1 activity, suggesting Nox1 activity is regulated by the phospholipase activity of Prdx6. Finally, wild type Prdx6, but not lipase or peroxidase mutant forms, supports Nox1-mediated cell migration in the HCT-116 colon epithelial cell model of wound closure. These findings highlight a novel pathway in which this antioxidant enzyme positively regulates an oxidant-generating system to support cell migration and wound healing.

Graphical Abstract

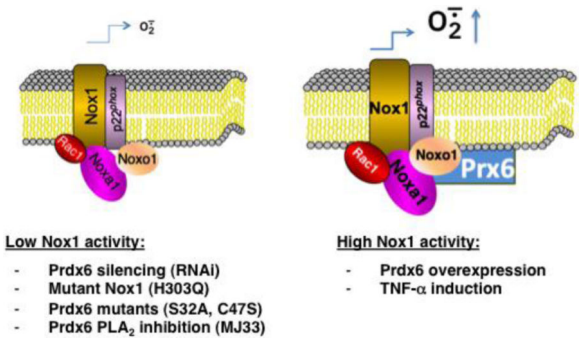

Keywords

Nox1; NADPH oxidase; Peroxiredoxin 6; Prdx 6; phospholipase A_2; peroxidase; cell migration

Introduction

Reactive oxygen species (ROS) are now regarded as important signaling molecules in biological systems and have diverse roles in health and disease. Along with mitochondria, a family of NADPH oxidase (Nox) enzymes has been identified as a major source of ROS in many cell types. These enzymes are membrane-integrated protein complexes that utilize molecular oxygen and NADPH to deliberately produce superoxide or hydrogen peroxide (H_2O_2). The human Nox family is composed of Nox1, Nox2, Nox3, Nox4, Nox5, Duox1, and Duox2.

Nox1 is most abundant in colon epithelial cells [1] and participates in mucosal innate immune responses, cell migration, wound healing, and epithelial homeostasis [2] [3] [4] [5] [6] [7] [8]. Nox1 is structurally most closely related to the phagocytic prototype, Nox2 (a.k.a., $gp91^{phox}$). Similar to Nox2, superoxide generation by Nox1 requires the membrane subunit $p22^{phox}$. Nox1 activation also depends on interactions with cytosolic regulatory cofactors, including Rac1[9] [10] [11], Nox organizer 1 (Noxo1), a $p47^{phox}$ adapter protein homolog, and Nox activator 1 (Noxa1), a $p67^{phox}$ activator protein homolog [12] [13]. The bis-SH3 domain of Noxo1 interacts with its C-terminal region containing its proline-rich

region (PRR); disruption of this interaction either by phosphorylation or arachidonate favors SH3 domain-mediated binding of Noxo1 to $p22^{phox}$ and promotes the PRR-mediated association with Noxa1 [9] [10] [14] [15] [16].

As inappropriate or excessive ROS production can damage surrounding tissues and promote inflammation, the activity of NADPH oxidases is subject to tight regulation. Nox2 remains dissociated and inactive in resting phagocytes until three major events occur during cell stimulation: 1) Rac activation through exchange of bound GDP for GTP, 2) phosphorylation of the cytosolic components, and 3) subsequent translocation of cytosolic components to the membrane, where they assemble with Nox2-$p22^{phox}$ heterodimers to form the active oxidase complex. The physiological agonists and molecular mechanisms that modulate activity of the Nox1 complex are not as well understood. Unlike Nox2, in some cells Noxo1 and Noxa1 are membrane-associated and Nox1 constitutively produces substantial amounts of ROS even in the absence of cell stimulation [9] [10] [12] [13] [15] [16]. Phosphorylation-dependent regulation of the Nox1 system has been described recently, through mechanisms that are distinct from those regulating Nox2 [17] [18] [19] [20] [21].

Previous studies found that peroxiredoxin (Prdx) 6 participates in activation of Nox2 in human neutrophils, alveolar macrophages, endothelial and other reconstituted cell models[22] [23] [24] [25]. Prdx 6 is a member of the ubiquitous antioxidant family of Prdxs with peroxidase activity that catalyzes removal of H_2O_2 and other hydroperoxides [26]. Prdx 6 is a 1-Cys peroxidase that utilizes glutathione (GSH) or ascorbate to recycle the oxidized form, whereas the other Prdxs require thioredoxin as the physiological reductant [26]. Prdx6 also differs from other mammalian Prdxs in its ability to reduce phospholipid hydroperoxides and in exhibiting phospholipase A_2 (PLA_2) activity [27]. An active site C47 is necessary for peroxidase activity, whereas a catalytic triad of S32-H26-D140 is needed for binding of phospholipid and PLA_2 activity [28]. One hallmark of oxidative stress is the peroxidation of unsaturated fatty acids in membrane phospholipids. Prdx6 can reduce phospholipid hydroperoxides such as phosphatidylcholine hydroperoxide with a relatively high rate constant similar to that of H_2O_2 reduction [29]. The Prdx6 PLA_2 activity catalyzes hydrolysis of the acyl group at the sn-2 position of glycerophospholipids, with specific affinity for phosphatidylcholine, to produce free fatty acids and a lysophospholipid [29]. While it has been generally assumed that the peroxidase activity of Prdx6 represents the main mechanism for its antioxidant function through its ability to remove oxidizing hydroperoxides and to repair peroxidized membrane phospholipids, the antioxidant effect of Prdx6 in *tert*-butyl hydroperoxide-treated PMVECs is dependent on both its peroxidase activity and PLA_2 activity[30]. Interestingly, the Nox2-supportive effect of Prdx 6 in whole cells appears to depend on its PLA_2 activity, but not its peroxidase activity [23, 24].

Several non-phagocytic Nox enzymes have demonstrated roles in cell migration or wound healing processes in epithelial and vascular tissues cells [2] [6] [31] [32]. Duox1 appears to participate in healing of chemically injured airway epithelium in responses involving EGFR signaling [33]. Nox4 and Nox1 promote tumor and vascular cell migration[8, 34-38]. Recently, the Nox1 enzyme complex was shown to direct colon epithelial cell migration and wound healing through formyl-peptide receptor mediated pathways previously described in phagocytic cells [2] [5] [6].

Here, we identify Prdx6 as a novel regulator of Nox1-based superoxide generation and cell migration, which appears to involve its PLA_2 activity. Prdx6 deficiency results in destabilization of other Nox1-supportive cofactors, whereas Prx6 overexpression supports higher levels of oxidase activity. These results highlight a novel pathway in which Prdx6 supports the oxidant-generating activity of Nox1 to promote cell migration. Based on these observations, we propose a model in which Prdx6 recruitment into the Nox1 complex adds another layer of post-translational control regulating the activity of this NADPH oxidase.

Materials and Methods

Materials

The following reagents were purchased as indicated: Diphenyleneiodonium chloride (DPI) and 1-hexadecyl-3-(trifluoroethyl)-*sn*-glycero-2-phosphomethanol lithium salt (MJ33) from Sigma-Aldrich (St Louis, MO, USA); recombinant human TNF-α from R&D Systems (R&D Systems, Minneapolis, MN); FuGENE6 from Roche (Roche, Indianapolis, IN, USA); Lipofectamine^{2000} from Invitrogen (Carlsbad, CA, USA). HA-Tag IP/Co-IP Kit and c-Myc Tag IP/Co-IP Kit were purchased from Pierce Biotech (Rockford, IL). The following antibodies were purchased as indicated: rabbit polyclonal anti-GAPDH Ab, rabbit polyclonal anti-myc from Sigma-Aldrich; mouse monoclonal anti-V5 Ab from Invitrogen; rabbit polyclonal anti-Nox1 Ab (NBP1-31546) from Novus Biologicals (Littleton, CO); rabbit polyclonal anti-Nox1 Ab-Agarose conjugate (sc-25545 AC), rabbit polyclonal anti-$p22^{phox}$ Ab-agarose conjugate (sc-20781), rabbit polyclonal anti-Cbl, rabbit polyclonal anti-Sos1, and rabbit polyclonal Prdx6 from Santa Cruz; Mouse monoclonal anti-HA Ab from Covance (Princeton, NJ, USA). Rabbit polyclonal Ab against Noxa1 (gift from Miklos Geiszt, Semmelweis University) and Mouse monoclonal Ab against $p22^{phox}$ (no. 449) were described previously [9]. pRS vector (#TR20003), GFP-specific shRNA vector (#TR30003), and four human Prx6-targeted pRS shRNA expression vectors (#TR310191) were obtained from OriGene (OriGene Technologies, Inc., Rockville, MD).

Yeast two-hybrid expression and screenings

Yeast two-hybrid based screening for potential binding partners of the SH3 domain of Noxa1 involved use of the Matchmaker System 3 (Clonetech Laboratories, Mountain View, CA), which employs GAL4 DNA-binding domain and activation domain fusion proteins produced by pGBKT7 and pGADT7 vectors, respectively, to detect protein-protein interactions in the yeast host strain AH109 [39]. All protocols for screening a human kidney cDNA library constructed in pGADT7 were performed according to manufacturer's recommendations. The cDNA fragment encoding the SH3 domain (residues 403-476) of Noxa1 was amplified by PCR and adapted for ligation into BamHI and NcoI sites of pGBKT7, the ‘bait’ vector. Western blotting confirmed production of a 30kDa HA-tagged fusion protein. Negative control experiments confirmed the absence of auto-activation (transcriptional false positivity) by plating of pGBKT7-Noxa1SH3 on selective SD/-Ade,-His,-Leu,-Trp medium. Verification of a positive interaction of the Noxa1 SH3 domain fusion protein with full-length Noxo1 (constructed in pGADT7) was confirmed by survival of AH109 on the same medium when co-transformed with both vectors.

Cell culture

All cell culture reagents were obtained from Invitrogen, unless indicated otherwise. Human HEK-293 cells (ATCC; American Type Culture Collection, Manassas, VA, USA) were maintained in Minimum Essential Medium (MEM)-α containing 10% heat-inactivated fetal bovine serum (FBS; HyClone/Thermo Scientific, Logan, UT) and antibiotics (100 units/ml penicillin and 100 μg/ml streptomycin) at 37°C in 5% CO2. Chinese hamster ovary (CHO-K1) cells (ATCC) were maintained in Ham's F-12 medium containing 10% heat-inactivated FBS and antibiotics at 37°C in 5% CO2. HT-29 cells and HCT-116 cells (ATCC) were grown at 37°C in 5% CO_2 in McCoy's 5A medium (modified) containing 10% heat-inactivated FBS and antibiotics.

Construction of plasmids

The cloning and construction of human Nox1, Noxa1, Noxo1-V5, and Myc-Noxa1 cDNA-encoding plasmids were described previously [9] [19]. The sequence for human Prdx6 (GenBank accession NM_004905.2) was amplified by PCR using fetal kidney first-strand cDNA (Stratagene) using primers targeted to the full-length coding sequence that were adapted with HindIII/XbaI sites for cloning into pcDNA3.1. N-terminal, HA epitope-tagged Prdx6 was amplified by PCR using primers adapted with HA-encoding sequence and the same restriction sites for cloning into pcDNA3.1. The Prx6 mutant S32A, C47S, D140A constructs, Nox1 mutant H303Q, and Noxa1 mutant W436R constructs were generated by PCR using the QuikChange site-directed mutagenesis kit (Stratagene, La Jolla, CA) according to the manufacturer's instructions. The sequences of all constructs were confirmed by DNA sequencing.

Transient transfections

HEK-293 and CHO-K1 cells were grown for 24 h in 6-well or 12-well plates (BD Biosciences, San Jose, CA, USA) and allowed to reach to 60-70% confluence in 2 ml or 1 ml of culture medium, respectively. Cells were transfected with pcDNA 3.1 plasmids encoding Nox1, Noxo1, Noxa1, and Prdx6 in the indicated combinations using the FuGene 6 transfection reagent (Roche Applied Science) according to the manufacturer's instructions. Transfection mixtures were incubated at room temperature for 20-min in OptiMEM (Life Technologies) and then added drop-wise to cells in normal culture medium. In studies expressing mutant Prdx6 or Nox1 components, equal amounts of plasmid were used in place of wild type. HCT-116 cells were transfected with Lipofectamine^{2000} (Invitrogen) as above, according to manufacturers' protocols. Briefly, 2.0×10^5 cells were seeded in 6-well tissue culture plates, 24h before transfection. Transfection DNA mixtures included Nox1, Noxo1 and Noxa1 and Prdx6 expressing plasmids (usually 2-2.4 ug total DNA), and in some control experiments Nox1 or Prdx6 plasmid was replaced by the same amount of GFP-expressing plasmid. Transient cell transfection rates typically exceeded 60 % at 48 hours post-transfection, as judged by live cell GFP fluorescence.

RNA interference-mediated silencing of Prdx6

HT-29 cells stably expressing human Prx6–targeted shRNAs (#TR310191), control GFP shRNA (#TR30003), and pRS-vector alone (#TR20003) were obtained by transfecting pRS-

shRNA vectors from OrigGene (OriGene Technologies, Inc., Rockville, MD) using Fugene 6, as above, followed by selection for antibiotic resistance. The following huPrdx6 sense 29-mer shRNA sequence was targeted: (#TI340760) 5′-GGATAGTGTGATGGTCCTTCCAACCATCC-3′. Following 48 hours transfection, diluted cells were grown in 10 cm plates in medium containing 3 μg ml^{-1} puromycin, and after 7–10 days single colonies were isolated and cultured. Cell lines with suppressed Prdx6 expression were qualified by anti-Prdx6 immunoblotting. For transient knockdown of Prdx6 in HEK-293, cell transfections were performed as described above, using 0.1 μg of Nox1, 0.1 μg of Noxa1, 0.1 μg of Noxo1, and 1.7 μg of pRS vector, GFP-specific shRNA vector, or human Prdx6-specific shRNA expression vector plasmid. Suppressed Prdx6 protein production was confirmed by immunoblotting, as described below.

Measurement of ROS

Extracellular superoxide release was detected by chemiluminescence using the superoxide specific Diogenes reagent (National Diagnostics, Atlanta, GA) with cells suspended in Hanks balanced salt solution (HBSS) with calcium and magnesium in the presence or absence of PMA (1 uM), as described previously [9]. Briefly, transfected cells were cultured for 48 hours (for plasmid DNA transfections) or 72 hours (for shRNA plasmid transfections), and then harvested by trypsinization at 37°C. After washing twice in HBSS by centrifugation (300×*g* for 5 min), cells were resuspended in HBSS containing calcium and magnesium at the desired cell densities, 2.5-5 × 10^5 viable cells/100-200 μl assay reaction. Kinetic chemiluminescence measurements were performed in 96-well opaque white plates at 37°C in a Luminoskan™ luminometer (Thermo, Waltham, MA, USA) at 30-60 second intervals over a time course of 20 minutes. Total integrated relative luminescence was calculated from all reactions preformed in triplicate assays. The observed Diogenes luminescence of all Nox1-expressing cell lines examined under these conditions was inhibited >96% by superoxide dismutase, was strictly dependent on co-expression of Noxo1 and Noxa1, and was linear with respect to cell number. In experiments examining inhibitory effects of MJ33 on Nox1-derived superoxide production, the inhibitor was dissolved initially in a dimethyl sulfoxide stock solution at 5 mM, which was then diluted directly into culture media of transfected cells to reach final inhibitory concentrations of 10-50 uM. Cells were then harvested by trypsinization for superoxide production assays either 1 or 9 hours after MJ33 addition, at 48 hours post-transfection.

Cell lysis, immunoprecipitation, and immunoblot analysis

Cell extracts were prepared in RIPA buffer (Boston Bioproducts, Worcester, MA, USA) supplemented with protease inhibitor cocktail (Sigma, St. Louis, MO, USA) by rocking for 30 min at 4°C and cleared by centrifugation (16,000 g, 10 min, 4°C). Protein concentrations were determined by the BCA method (Pierce, Rockford, IL, USA). For immunoprecipitation studies, washed cells were lysed with cold 1% Nonidet P-40 buffer (Boston Bioproducts, Ashland, MA, USA) supplemented with protease inhibitor cocktail (Sigma) by rocking for 15 min at 4°C. Cleared supernatants were incubated overnight (4°C) with the indicated antibodies to capture immune complexes. After three washes in lysis buffer, bound proteins were eluted in SDS-sample buffer (Invitrogen) and subjected to SDS-PAGE analysis. Cell

lysis, immunoprecipitations, and Western blotting analysis were performed as previously described [40].

Cell migration assays

Quantifying cell migration and proliferation using image-based microscopy to measure changes in the gap morphology is a widely used cell assay for studying a variety of functional properties in normal or cancerous cells across scale from genomic to tissue level [41]. The transfected HCT-116 colon epithelial cells form monolayers with cell migration to close the silicone culture insert- (also referred to as stencil- or fence-) induced gap without piling up. However, the majority of the quantitative parameters to characterize the cell-free gap between cell margins such as average gap width, maximum gap width, area or margin smoothness are measured manually or semi-automatically, which limits their reproducibility and effectiveness for large scale high-throughput studies, especially when manual scratch wounds are used that can vary between experiments and labs. A key advantage of the proposed quantitative endpoint gap measurement used in this study to characterize cell migration is that it is fully automatic and non-invasive. Only the endpoint is measured so there is no live cell staining and time-lapse imaging, which could perturb cell behavior.

Six hours after co-transfection with Prdx6 and Nox(1, -a1, -o1) expression vectors, HCT-116 cells were trypsinized and reseeded into triplicate silicone culture inserts (Ibidi LLC, Verona, Wisconsin, USA) mounted onto collagen1-coated 12-well culture plates, which create dual chambers separated by a 0.5 mm cell-free boundary. Briefly, 70μl of cells suspended in complete McCoy's 5A medium (1×10^6 cells/ml) were applied to each chamber, allowed to adhere over 24 hours, and formed a nearly confluent monolayer. The silicone frames were then removed, thereby creating a reproducible gap between boundaries formed by cell monolayers within the two chambers. The cells were allowed to migrate into the gap areas for 20 hours, reaching a maximum endpoint of ~70% closure before being fixed with methanol and stained with Eosin Y and Azure B (Diff Stain Kit, IMEB Inc., San Marcos, CA, USA).

Cell migration data were collected and processed from three independent transfection experiments. Replicate transfections were performed for assays of superoxide production, cell proliferation, and Western blot analysis performed in parallel 48 hours post transfection. Consecutive visible light images of the fixed and stained migrating cells, using a Zeiss Axiovert10 microscope (10X objective lens) and Spot imaging software (Diagnostic Instruments, Sterling Heights, MI), were collected along the entire length of the gaps and then processed to determine migratory distances among various transfected cell groups.

Gap Closure Index (GCI)

A three-step process was used to quantitatively estimate the amount of cell migration by measuring the change in the gap area (cell-free region) using the gap closure index (GCI). For the initialization step, the left and right gap boundaries were located on an image row-by-row basis by maximizing the Line Gap Energy (LGE) using the following definition of gap energy E_G:

$$E_G = E_I^{\alpha} \cdot E_W^{\beta} \cdot E_S^{\gamma} \quad (1)$$

where the energies E_I, E_W, E_S are related to the color intensity, width, and smoothness of the gap, respectively. The parameters α, β γ weight the three energies and influence the quality of the estimated left and right cell margins. For the experiments shown these parameters were experimentally chosen as follows: $\alpha = 0.75$, $\beta = 0.05$, $\gamma = 0.2$. For each possible left/right boundary pair candidate in an image row, the gap energy E_G is computed, and the pair with the maximum energy is chosen as the most likely gap boundary for this row. The energy term E_I compares the pixel intensities within and outside the candidate boundaries with the typical background color (gap color). This energy reaches its maximum when the pixel colors within the candidate boundaries are identical to the background color, and the pixel colors outside the candidate boundaries are dissimilar from the background color. The energy term E_W represents the relative width of a candidate gap. It reaches its maximum for a gap that covers an entire row of a microscope image. The last energy term, E_s, represents the smoothness of the gap. It reaches a maximum when the gap boundaries in one row are identical to the left/right boundaries in the neighboring rows. To speed up computation, the gap energy E_G is maximized independently on a row-by-row basis.

In the second step, the convex gap margin boundaries produced by the LGE method are further smoothed and refined, tracing non-convex regions, using geodesic active contour evolution based on a level set formulation [42] [43]. The background masks obtained in the first step are eroded to provide an initial contour inside the gap area from which a level set is expanded by an adaptive force until stopped by the margins of the gap. The contours are represented implicitly by a level set function, which is evolved using a partial differential equation speed function. The edge stopping function is inversely proportional to edge strength to prevent active contours from crossing the leading edge. Migrating cell boundaries obtained from the geodesic active contour evolution are morphologically processed to produce a wound gap mask from which the CGI can be computed.

In the final step, we use the foreground image region estimated from the active contour process to compute the GCI at the end-point time T, using the following formula:

$$GCI = 1 - \frac{G_T}{G_0} \quad (2)$$

where G_T is the gap size computed at the end-point time T, and G_0 is the initial starting point gap size at $T = 0$. A GCI of 0, 0.5, or 1 indicates that the gap has not changed and is identical in area to the initial gap, has closed 50%, or has fully closed at time T, respectively. Automated image analysis for estimating the GCI is robust since neither cell tracking nor cell margin (tissue) tracking is necessary in the end point gap closure method; such tracking methods are computationally more complex with higher variance depending on the experimental and imaging conditions [44] [45] [46].

Results

Prdx6 associates with the Noxa1 SH3 domain of Noxa1 and stabilizes Noxa1

Previous studies showed the Nox1-supportive organizer protein, Noxo1, exhibits an expression pattern similar to that of Nox1, whereas the Noxa1 activator protein is distinct in showing high expression in tissues other than colon[13] [15]. In efforts aimed at understanding regulation of Nox1 and related multi-component NADPH oxidases, we screened for other candidate regulators that bind to the SH3 domain of Noxa1. In yeast two-hybrid expression experiments using the Noxa1 SH3 domain (codons 403-476) as “bait” in the pGBKT7 vector, we screened a library of ~500,000 human kidney cDNAs constructed in pGADT7, as described in the “Methods” section. Among several potential targets initially identified under low stringency screening through selection of co-transformants on SD/-Leu/-Trp medium, we identified one pGADT7 clone encoding a partial sequence of Prdx6 (codons 78-224) that enabled survival of yeast strain AH109 on SD/-Ade/-His/-Leu/-Trp plates when co-expressed with the Gal4 DNA binding protein fused with the SH3 domain of Noxa1 (Fig 1A). These co-transformants also tested positive for αgalactosidase activity, providing further evidence of an interaction supporting GAL4 transcriptional activation in yeast.

Binding of Prdx6 to the SH3 domain of Noxa1 suggests Prdx6 could associate with the assembled Nox1 complex in which Noxa1 serves as a critical activator. To explore this possibility, we developed several mammalian cell models to confirm the interaction of the full length Noxa1 and Prdx6 proteins. HEK-293 and CHO-KI cell lines exhibited Nox1 oxidase activity through transient co-transfection of Nox1 components (Nox1, Noxa1, and Noxo1). HCT116 and HT-29 lines were chosen as human colon epithelial models; HT-29 cells show endogenous Nox1 expression and superoxide release [3] [13] [47].

In initial experiments HEK-293 cells were co-transfected with Nox1, Noxa1, and Noxo1 along with or without HA-tagged Prdx6. Cell lysates from these transfectants were immunoprecipitated to pull down endogenous $p22^{phox}$ immune complexes using an agarose-conjugated $p22^{phox}$ antibody. Western blot results showed a strong association between $p22^{phox}$ complexes and HA-Prdx6, along with V5-Noxo1 and Myc-Noxa1 (Figure 1B) suggesting Prdx6 interacts with the Nox1 complex.

To examine further how Prdx6 associates with Noxa1, a series of transient transfections and immunoprecipitation experiments were performed with CHO-KI cells. In the first experiment, we introduced a mutation in Noxa1 at tryptophan-436 (W436R), which represents a highly conserved residue in the core, ligand-binding pocket of all SH3 domains that was shown to disrupt Noxa1 binding to the C-terminal, proline-rich region of Noxo1 and inhibit translocation of Noxa1 to the membrane [9] [16]. CHO-K1 cells were co-transfected with increasing amounts of HA-tagged Prdx6-encoding plasmid along with a fixed amount of either wild type (WT) Noxa1 plasmid or mutant W436R Noxa1 plasmid. Lysates from these transfected cells were harvested 48 hours later and analyzed by Western blotting. Transfection with increasing amounts of HA-Prdx6 plasmid along with wild type (WT) Noxa1 plasmid not only resulted in increased production of HA-Prdx6, but also led to

increased detectable amounts of Noxa1. This pattern of enhanced Noxa1 protein levels was not observed in cells transfected with mutant W436R Noxa1 (Fig. 1C).

In a second experiment, HA-Prdx6 immunoprecipitation from 48-hour transfected culture lysates with agarose-conjugated anti-HA antibody was analyzed by western blotting with anti-Noxa1 antibody. WT Noxa1 was found associated with the Prdx6 complexes in amounts that correlated with increasing amounts of Prdx6 (Fig. 1, right). However, the W436R Noxa1 mutant was not associated with the precipitated Prdx6 complexes. This result suggests Prdx6 associates with and stabilizes Noxa1 and that the conserved tryptophan-436 within the core, binding surface of the Noxa1 SH3 domain is critical for its association with Prdx6.

Similar experiments were performed in HEK-293 cells. Cell lysates from transient (48 hour) co-transfections with increasing amounts of HA-tagged Prdx6 plasmid and fixed amounts of either Myc-tagged WT Noxa1 or W436R Noxa1 plasmids were prepared and analyzed. As shown in Fig. 1D, increased expression of HA-tagged Prdx6 led to increased detection of wild type (WT) Myc-tagged Noxa1, as in the case of CHO-K1 cells. In contrast, the SH3 domain mutant protein, Noxa1 W436R, did not exhibit the same pattern as WT: Noxa1 W436R protein levels were much lower than that of WT Noxa1 and did not support higher levels of Prdx6 co-expression.

To confirm that the SH3 domain of Noxa1 is critical for its association with Prdx6, Noxa1 immunoprecipitation with agarose-conjugated Myc antibody was performed on cell lysates of HEK-293 cells transfected with WT or W436R Myc-Noxa1 along with or without HA-Prdx6. HA-Prdx6 showed a strong association with WT Noxa1, whereas HA-Prdx6 was not associated with W436R Noxa1 precipitates (Fig. 1E). Taken together, the results of Fig. 1B-E indicate that Prdx6 associates with WT Noxa1 through the SH3 domain of Noxa1 and has a strong stabilizing effect on Noxa1 protein levels in both cell models.

Prdx6 augments superoxide generation by Nox1

The association of Prdx6 with the Nox1 complex suggests Prdx6 may have modulating effects on superoxide generation by Nox1. In previous work we showed that several cell models co-transfected with human Nox1, Noxo1, and Noxa1 constitutively produce extracellular superoxide, which is readily detected by SOD-sensitive Diogenes luminescence [9] [13]. HEK-293 cells with high levels of endogenous Prdx6 were transiently co-transfected with a Prdx6-targeted shRNA (TI340760) along with Nox1, Noxo1, and Noxa1 cDNAs. Endogenous Prdx6 protein levels were significantly reduced in these cells when compared with cells transfected with empty vector (pRS) or with GFP-targeted shRNA (GFP) (Fig. 2A). Transfection with the Prdx6-targeted shRNA (Prdx6) led to reduced superoxide generation when compared with the control transfectants. Similar results were observed in HT-29 cells. In this case, stable HT-29 clones generated by transfection of Prdx6-targeted shRNA showed much lower Prdx6 protein levels when compared with control pRS or GFP-targeted shRNA transfectants (Fig. 2B). The reduced-Prdx6 HT-29 clones also produced significantly lower extracellular superoxide in comparison with the control cell lines. These data suggest that Prdx6 positively regulates Nox1 activity.

The reciprocal approach of overexpressing Prdx6 in human Nox1-reconstituted CHO-K1 cells provided further support for Prdx6 functioning as a Nox1-supportive cofactor. CHO-K1 cells were transfected with fixed amounts of Nox1, Noxo1, and Noxa1 plasmid along with increasing amounts of HA-Prdx6, and extracellular superoxide generation was measured 48 hrs later. Co-transfection with Prdx6 led to dose-dependent increases in the production of extracellular superoxide (Fig. 2C). Western blot analysis showed that these higher Prdx6 levels led to enhanced detection of the soluble Nox1-supportive factors, Noxo1 and Noxa1. This suggests that Prdx6 has a positive effect on Nox1-based superoxide generation by influencing the stability of Noxo1 and Noxa1 proteins.

Both PLA_2 and peroxidase mutant forms of Prdx6 fail to support Nox1 activity

To investigate the basis of the apparent supportive effects of Prdx6 on the Nox1 system, we generated several Prdx6 mutants affecting its enzyme activities. Prdx6 is a bi-functional enzyme known to possess two distinct activities: acidic, calcium-independent phospholipase A_2 activity and glutathione peroxidase activity. Serine-32 in the PLA_2 active site was substituted with alanine in the S32A Prdx6 mutant, whereas the D140A mutant was also shown to exhibit impaired PLA_2 activity without affecting phospholipid substrate binding [28]. To abolish the peroxidase activity of Prdx6, the active site cysteine-47 was mutated to serine. Co-transfection with the Prdx6 S32A mutant along with the Nox1, Noxo1, and Noxa1 led to much lower superoxide generation in CHO-K1 cells when compared with cells expressing WT Prdx6 (Fig. 3A). The D140A PLA_2 mutant supported even lower Nox1 activity in comparison with WT Prdx6. Co-transfection of the C47S peroxidase mutant also supported lower Nox1-derived superoxide generation than WT. Western blotting detected the S32A and C47S mutant proteins at levels greater than or equal to that of the WT, whereas the D140A protein appeared to be considerably less stable. All Prdx6 mutant proteins appear to support lower production of co-transfected Noxo1 and Noxa1 proteins. Figures 3B and C show that co-transfection with increasing amounts of S32A or C47S Prdx6 along with WT Prdx6 led to dose-dependent decreases in detectable Noxo1 and Noxa1 protein levels; this correlated with proportionately lower superoxide yields. To confirm these observations in a Nox1-expressing colon epithelial cell model, we transfected WT or mutant HA-Prdx6 along with Noxo1 and Noxa1 into HT-29 cells. Cells overexpressing WT Prdx6 showed enhanced superoxide release in response to PMA, whereas cells expressing the mutant forms produced less superoxide (Figure 3D). These results indicate that both the PLA_2 and peroxidase activities of Prdx6 may be involved in supporting higher Nox1 activity and may contribute to Prdx6-based stabilization of Nox1 components. Furthermore, it appears that the mutant proteins can have suppressive effects in cells co-transfected with WT Prdx6.

TNF-α regulates Prdx6 and Nox1 expression and the association of Prdx6 with the Nox1 complex

TNF-αis known to induce both Nox1 and Noxo1 expression [48] [49]. We examined the association of Prdx6 and the Nox1 system in response to TNF-α treatment in HEK-293 cells that were co-transfected with Prdx6 along with Nox1, Noxo1, and Noxa1 for 40 hrs. After TNF-α treatment, cells were harvested at various times up to 9 hrs for extracellular superoxide measurements, and cell lysates were prepared for Western blot analysis and immunoprecipitation experiments. TNF-α treatment induced increased superoxide

generation in this Nox1-reconstituted model, which closely correlated with enhanced detection of Prdx6, Noxo1, and Noxa1 proteins observed within two phases (Fig. 4A and B). Around 3 hrs after TNF-α treatment, events related to new transcription and translation may support greater Noxo1, Noxa1, and Prdx6 protein stability or inhibit their degradation, since the expression vectors encoding these proteins are not directly responsive to TNF-α. To test whether Prdx6 is associated with the Nox1 enzyme complex after TNF-α treatment, Nox1 was immunoprecipitated with agarose-conjugated Nox1 antibody and the associated Prdx6 was probed with anti-HA antibody. TNF-α induced an association of Prdx6 with Noxo1 detected after 5 hours treatment (Fig. 4C), while the association of Prdx6 in Nox1 immunoprecipitates also was enhanced in parallel (Fig. 4D). Taken together, these data show that TNF-α stimulates higher Nox1 activity through an induction of the Nox1-supportive cytosolic components and Prdx6, while promoting the association of Prdx6 with the Nox1 complex.

Prdx6 PLA_2 and peroxidase mutants support lower Nox1 activity in TNF-αinduced cells

To investigate the involvement of Prdx6 in TNF-α-induced superoxide generation by Nox1, HEK-293 cells were co-transfected with various constructs of Prdx6 along with Nox1, Noxo1 and Noxa1 (40 hours) and then stimulated with TNF-α for 6 hrs. Extracellular superoxide generation from cells treated for 6 hours was increased in cells co-transfected of WT Prdx6, but not in cells expressing the PLA_2 mutant (S32A) or the peroxidase mutant (C47S) Prdx6 (Fig 5A). Analysis of proteins detected in cell lysates showed that WT Prdx6 has a positive impact on TNF-α induction of transfected Noxo1 and Noxa1 proteins, whereas detectable levels of these factors were diminished with PLA_2 or peroxidase Prdx6 mutant transfections (Fig 5A). Thus, only WT Prdx6 influences TNF-α-dependent induction of the Nox1 system, even when produced by expression vectors that are not directly TNF-α responsive. When WT or S32A Prdx6 was immunoprecipitated from cell lysates prepared from TNF-α treated cells, the association of S32A Prdx6 with Noxo1 was found to be significantly reduced (Fig 5B). When HEK-293 cells were co-transfected with increasing amounts of Prdx6 along with Nox1, Noxo1, and Noxa1, WT Prdx6 supported increased production of Noxo1 protein in a dose-dependent manner, whereas transfection of PLA_2 mutant S32A did not enhance Noxo1 levels as observed with WT Prdx6 (Fig 5C). These data suggest that the TNF-α stimulated increase of superoxide generation occurs through interaction of WT Prdx6 with Nox1 components, leading to increased levels of Nox1 components and Prdx6.

Inhibition of Prdx6 PLA2 activity suppresses Nox1 activity

The above findings suggest the suppressive effects of Prdx6 mutagenesis on Nox1 reconstitution could be attributed solely to structural changes induced by mutations that disrupt Prdx6 interactions with Nox1 components, rather than being a consequence of the loss of Prdx6 enzymatic activities. In order to independently assess possible involvement of Prdx6 PLA2 activity in Nox1 activation, we examined the effects of the competitive PLA2 inhibitor, MJ33, which is relatively specific for Prdx6 that exhibits low toxicity on living cells [23] (and refs. therein). We explored a range of MJ33 treatment times and concentrations in three Nox1-reconstituted cell models (Figure 6), from 1 hour (HCT-116 and HEK-293 cells; 10-50 uM MJ33) to 9 hours (CHO-K1 cells; 10-20 uM MJ33) prior to

cell harvesting for oxidase assays. The HCT-116 colon epithelial cell line transfected (48 hours) with Nox1, Noxo1, Noxa1 and Prdx6 (WT or mutant forms) showed the highest levels of Nox1 activity when WT Prdx6 was expressed (Fig 6B), similar to that observed in the three other Nox1-transfected cell lines. Incubation of these cells with MJ33 (1 hr) caused a significant dose-dependent inhibition of PMA-stimulated Nox1-derived superoxide generation. Inhibition was greatest in WT Prdx6-expressing cells, approaching 70% inhibition of Nox1 activity at 50 uM MJ33, whereas the relative extent of Nox1 inhibition by MJ33 observed in cells expressing the phospholipase or peroxidase mutant forms of Prdx6 was lower. These same trends were also observed in Nox1-reconstituted HEK-293 cells (data not shown), whereby WT Prdx6 expressing cells showed a higher relative dose-dependent MJ33 inhibition profile of Nox1 activity when compared with mutant Prdx6-expressing cells. In other experiments we investigated the effects of long-term (9-hr) MJ-33 treatment on Nox1 activity in transfected CHO-K1 cells and observed up to 40% inhibition of constitutive Nox1-derived superoxide release by 20 uM MJ33 (Figure 6C). The 9-hour treatments had no significant effects on cell viability or the levels of Prdx6 or other Nox1-supportive proteins detected by Western blotting. Taken together, these findings indicate that MJ33 inhibition of Nox1 activity most likely occurs through its inhibition of Prdx6 PLA_2 activity, as was concluded from similar experiments exploring Nox2 activation by Prdx6 in pulmonary vascular endothelial cells [23].

Nox1-derived reactive oxygen species generation stabilizes the Nox1 system through Prdx6

It has been shown that *PRDX6* gene expression is regulated by oxidative stress, suggesting that Nox1-derived ROS could enhance Prdx6 production [50]. Our results (Figs. 2, 3 and 4) indicate that Prdx6 can, in turn, support higher Nox1 activity, because the stability of the Nox1 system appears to depend on its association with active Prdx6. Thus, it is possible that Nox1-derived ROS generation regulates Prdx6, leading to stabilization of the Nox1 system in a positive feedback cycle. In order to explore effects of Nox1-derived ROS generation on its own stability, we engineered a defective mutant of Nox1 modeled after a Nox2 mutation detected in the X-linked form of chronic granulomatous disease, by the substitution of a putative heme-binding histidine-303 with tryptophan (H303Q)[51]. Transfection of various amounts of Nox1 H303Q demonstrated a superoxide-generating capacity that was less than 10 % of the transfected WT Nox1 (Fig 7A). The levels of Myc-Noxa1 and HA-Prdx6 detected by Western blotting of cells co-transfected with Nox1 H303Q were substantially reduced in comparison with cells expressing WT Nox1 (Fig 7B). When increasing amounts of this Nox1 mutant were co-transfected with the complete Nox1 system and HA-Prdx6, there were suppressive effects on extracellular superoxide generation by WT Nox1 (Fig 7C). Furthermore, the levels of Prdx6 and Noxo1 proteins were significantly reduced by co-transfection of mutant Nox1 (Fig 7C). These results suggest this mutant has dominant-negative effects on WT Nox1 and that Nox1-derived superoxide generation has a positive influence in stabilizing components of the Nox1 system as well as Prdx6.

Prdx6 supports Nox1-dependent colon epithelial cell migration

Several reports indicate Nox1 supports migration of colon epithelial and vascular cells [2] [6] [31] [32]. Thus, we examined the effects of Prdx6 on Nox1-dependent migration in

HCT-116 colon epithelial cells. Unlike HT-29 cells, which produce some endogenous Nox1-derived ROS, the transformed HCT-116 colon epithelial line exhibits a lower background of ROS generation. Also, HCT-116 cells have been used extensively in cell migration studies and are easily transfected, allowing efficient reconstitution of Nox1 activity in this model. Cells were transfected 6 hours and then reseeded into dual Ibidi chambers for 24 hours. Once they formed monolayers at a nearly confluent state, the frames were lifted to initiate cell migration into the denuded area between chambers. Transfection of HCT-116 cells with the complete Nox1 system (Nox1, Noxo1 and Noxa1) along with WT Prdx6 resulted in greatly enhanced migratory behavior, exhibiting ~70% closure of a 0.5 mm gap between cell boundaries within 20 hours (Fig 8B, C). In contrast, transfection of the Nox1 system in the absence of overexpressed WT Prdx6 significantly compromised cell migration (2 *vs.* 1). Nox1-reconstituted cells overexpressing PLA_2 or peroxidase mutant forms of Prdx6 (S32A or C47S) exhibited even less migratory activity (3 or 4 *vs.* 2). Furthermore, transfected cells in which Nox1 was omitted or substituted with the defective Nox1 H303Q mutant also exhibited significantly reduced migratory behavior even in the presence of overexpressed WT Prdx6 (5 and 6). The reconstituted HCT-116 cells exhibited the same effects of overexpressed Prdx6 on Nox1 activity (Fig 8D) that was observed in the HT-29 and HEK-293 cell models (Figs 3 and 5): WT Prdx6 enhanced basal Nox1 activity, whereas PLA_2 and peroxidase mutants failed to support higher Nox1 activity. Parallel experiments comparing total cell counts 48 hours post-transfection detected a slight increase in cell numbers the in cultures co-expressing WT Nox1 and Prdx6 (~15%) relative to the other 5 transfections (data not shown), suggesting that enhanced Nox1 and Prdx6 activities primarily affects cell migration, not proliferation, in this model. Western blotting of transfected HCT-116 cells also confirmed some of the same effects seen in the other cell models, including detection of lower levels of WT Prdx6 and Noxo1 in the absence of WT Nox1 (Fig 8E). Taken together, these findings indicate that Prdx6 not only supports Nox1 production of superoxide, but also contributes to Nox1-mediated cell migration of this colon epithelial cell model.

Discussion

Prdx6 is unique among members of the Prdx antioxidant family because it exhibits both glutathione peroxidase and phospholipase A2 activities and has only one catalytic cysteine [27]. Our current studies show Prdx6 positively regulates Nox1-based superoxide generation in several cell models and that Prdx6 supports Nox1-dependent migration of the colon epithelial tumor line, HCT-116. Initially, we demonstrated that Prdx6 binds to Noxa1 in yeast two-hybrid screening experiments aimed at identifying novel Noxa1 SH3 domain-binding partners. Then, we showed Prdx6 binds to full-length Noxa1 through its SH3 domain and associates with the assembled Nox1 complex in several cell models. Experiments manipulating cellular Prdx6 levels confirmed a close association between Prdx6 and at least two other Nox1 components (Noxa1 and Noxo1) by showing that RNA interference-mediated suppression of Prdx6 production also reduced Noxa1 and Noxo1 levels and diminished Nox1 activity. In addition, Prdx6 overexpression led to higher levels of these Nox1 components and higher superoxide generation. Furthermore, we showed that TNF-α induction stabilizes higher levels of Prdx6 along with Noxa1 and Noxo1, even when

expressed using vectors that are not specifically responsive to this cytokine. Beyond demonstrating the association and co-stabilization of other Nox1 components, we showed the Nox1-supportive effects of Prdx6 may involve both its glutathione peroxidase and PLA_2 activities, in that the mutated, catalytically inactive forms of Prdx6 fail to support higher Nox1 activity or Nox1-dependent cell migration when compared with WT Prdx6. These inactive mutants exhibited impaired binding and stabilization of other Nox1 components seen with WT Prdx6. However, further evidence supporting the involvement of Prdx6 PLA2 activity in Nox1 activation was obtained by showing that the competitive phospholipase inhibitor, MJ33, suppressed WT Prdx6-dependent Nox1 activitys in PMA-stimulated and non-stimulated cell while not affecting detectable levels of Prdx6 or other Nox1-supportive components. These findings are outlined in the scheme shown in Figure 9, which speculates on how the activities and levels of Prdx6 and Nox1 components are closely linked.

Prdx6 regulation of NADPH oxidase activity was described earlier in the case of Nox2, the closest homologue of Nox1. Leavey, et al., first showed Prdx6 interacts with 67^{phox}, the homologue of Noxa1, and supports amphiphile-dependent Nox2 activity in a cell-free reconstituted assay [25]. Later studies on Nox2 activation in whole cell and mouse model systems, however, revealed an important distinction from our Nox1 findings, in that the Nox2-supportive effects of Prdx6 are critically dependent on its phospholipase A_2 activity, but are apparently independent of its peroxidase activity. The Fisher lab showed this PLA_2 activity is required for angiotensin II-mediated activation of Nox2 NADPH oxidase in mouse pulmonary microvascular endothelial cells (PMVEC), as well as in stimulated alveolar macrophages [23]. Transfection of Prx6 null mouse PMVEC with WT or C47S (peroxidase-mutant) Prdx6, but not with PLA_2 active site mutants (S32A, H26A, and D140A), rescued angiotensin II-induced PLA2 activity and ROS generation. Similar results were obtained in Prdx6-deficient, differentiated PLB-985 myeloid cells, where reconstitution with the PLA_2 activity of Prdx6 was necessary for maximal oxidase activity of Nox2 in response to the bacterial peptide formyl-methionylleucyl-phenylalanine (fMLF), but not PMA [24]. Other experiments showed acute lung injury caused by ischemia-reperfusion, LPS or hyperoxia exposure was prevented by blocking Nox2 activation by using the transition state analogue inhibitor of Prdx6 PLA_2 activity (MJ33), which does not affect the antioxidant (peroxidase) function of Prdx6 [52] [53] [54]. Thus, despite the well-established role of Prdx6 in antioxidant defense, the paradox of how Prdx6 *promotes* oxidative stress in the context of acute lung injury was explained on the basis of its independent phospholipase function, which activates Nox2. Interesting, these studies saw no inhibitory effects of MJ33 on Nox1 activation by angiotensin II in vascular smooth muscle cells [52], whereas we observed Nox1 inhibition by MJ33 in three models (both PMA-stimulated and unstimulated cells). The basis for the apparent differences between Prdx6 activation of the Nox2 and Nox1 systems, where our observations in several models showed that both PLA_2- and peroxidase-defective mutants of Prdx6 failed to support Nox1 activity as well as WT Prdx6, may reflect intrinsic differences in host cell systems, differences of various agonist-specific signaling pathways, or compensation by other antioxidant pathways unique to each cell system.

Earlier studies showed Nox2 activation in phagocytes can depend on another phospholipase, p85 $cPLA_2$, and that exogenous arachidonic acid restores Nox2 activity in PLB-985 cells

deficient in $cPLA_2$ [55]. Other studies on cPLA2 knockout mice suggested this phospholipase had no role in Nox2 activation [56], consistent with the dependence of murine Nox2 on the phospholipase A2 activity of Prdx6. Arachidonate and other soluble amphiphiles activate cell-free reconstitution of Nox2 and may act in promoting assembly and activation of Nox2 in whole cells by inducing structural changes in $p47^{phox}$ and $p67^{phox}$ that enable their interaction with membrane oxidase components, $p22^{phox}$ and Nox2, respectively [57] [58]. Arachidonate or sodium dodecyl sulfate can also induce changes in Noxo1 that promote its interaction with $p22^{phox}$ [14] [16]. Therefore, future work should investigate whether Prdx6 PLA_2-derived lipid metabolites (free fatty acids and lysophosphosphatidyl choline) mediate Nox1 or Nox2 activation.

Our demonstration of a direct association between the Noxa1 SH3 domain and Prdx6 implies that the C-terminal SH3 domain of $p67^{phox}$ could bind to Prdx6 in a similar fashion. Earlier studies showed the C-terminal SH3 domains of $p67^{phox}$ and Noxa1 bind to $p47^{phox}$ and Noxo1, respectively, and are required for their recruitment to the membrane [9, 16, 59]; whether Prdx6 competes or cooperates with these interactions is currently unknown. It appears that Prdx6 also has stabilizing effects on the Nox2 complex: it increases the V_{max} of the enzyme in *in vitro* assays and supports translocation and retention of $p67^{phox}$ and $p47^{phox}$ with Nox2 on the membrane of whole cells [22]. One recent study showed binding of $p67^{phox}$ to Prdx6 suppresses its PLA_2 activity, suggesting this interaction could either inhibit oxidase activation until assembled with other components or mediate the termination of ROS production [60]. Future studies should explore how the formation of a ternary oxidase complex with Prdx6 affects the turnover of other Nox1 or Nox2 components and determine when these interactions occur in the sequence of oxidase assembly, activation or termination.

Few studies to date have described post-translation regulation of Nox enzyme activity through protein degradation-based mechanisms. Two reports linked diminished ubiquitin-dependent degradation of Nox components ($p22^{phox}$ and Rac1) and elevated Nox-derived ROS production to the absence of tumor suppressors (VHL and HACE1, respectively) as a basis for tumorigenesis [61] [62]. Our observations indicate that ROS produced by Nox1 may provide a positive feedback signal that stabilizes higher levels of Noxo1, Noxa1, and Prdx6 (Figure 7). We showed expression of the low-activity Nox1(H303Q) mutant results in lower levels of all three Nox1-supportive proteins, lower superoxide output, and diminished cell migration. The potential cellular targets of Nox1-derived oxidants that result in enhanced stabilization of Nox1 proteins and higher oxidative output are currently unknown and are under investigation. They may include components of the ubquitin-proteosome machinery, since critical enzymes in ubiquitin-dependent protein degradation pathways have cysteine at their active sites that can be oxidatively inactivated [63]. Alternatively, Prdx6 itself may represent a key susceptible target of oxidation, as it associates with the source of ROS in this case, consistent with models of oxygen sensing functions of Prdx in other systems where they serve to relay intracellular redox signals [26]. Such a model is supported by our observations with the non-oxidizable (peroxidase deficient) mutant (Prdx6 C47S), which also fails to bind to and stabilize Nox1 components or support higher Nox1 activity. Interestingly, one study showed that hyperoxidation of Prdx6 at C47 greatly enhanced its PLA_2 activity [64], which could explain how Nox1-derived ROS can affect higher oxidative

output in a positive feedback loop involving C47 oxidation effects on the PLA_2 activity of Prdx6. Alternatively, it is known that oxidative stress induces Prdx6 expression via the Nrf2 pathway because the Prdx6 promoter contains antioxidant response elements [50]. Thus, Nox1-derived ROS generation may induce higher Prdx6 expression through the Nrf2 pathway, thereby providing another feed-forward mechanism for stabilization of Nox1 components and higher oxidase function. Further studies are needed to confirm these mechanisms.

In summary, we have detected multiple effects of Prdx6 on the Nox1-based NADPH oxidase in several cell models (Fig. 9): WT but not mutant forms (S32A, C47S) of Prdx6 bind to and co-stabilize higher levels of the Nox1-supportive components (Noxa1 and Noxo1), leading to higher Nox1 oxidase activity even in the absence of cell stimulation. Other evidence based on experiments using the PLA_2 inhibitor MJ-33 suggests direct involvement of the PLA_2 activity of Prdx6 in Nox1 activity independent of any alterations in the levels of Nox1-supportive components. The latter effects of Prdx6 PLA_2 activity may involve generation of lipid products (lysophosphatidyl choline or free fatty acids) that promote optimum oxidase component interactions or activation, as suggested with the Nox2 enzyme [23] [24].

In conclusion, our identification of a functional interaction of Prdx6 with Nox1 provides further insight on post-translation regulation of this oxidase that may be relevant to proposed physiological and pathological roles of Nox1 in vascular, epithelial, and tumor tissues. Several reports described involvement of Nox1 in cell proliferation, migration, and wound healing [2] [3] [5] [6] [38], one involving arachidonate metabolism [8], although Prdx6 was not implicated in these studies. Interestingly, other reports suggest the $iPLA_2$ and peroxidase activities of Prdx6 promote tumor growth and metastasis, although involvement of Nox1 was not explored in these studies [65] [66] [67]. It will be critical in future work to determine whether these processes relate to the functional partnership of Nox1 with Prdx6, which may suggest novel approaches for therapeutic intervention.

Acknowledgements

This work was supported by funds from the Intramural Research Program of the NIH, National Institute of Allergy and Infectious Diseases (ZO1-AI-000614) and, in part, by research funds from Chungnam National University. The authors are grateful to Dr. Miklos Geiszt (Semmelweis University) for providing antibodies against Noxa1 and Dr. Gary M. Bokoch (deceased, Scripps Research Institute) for providing the Myc-tagged Noxa1cDNA.

References

1. Suh YA, Arnold RS, Lassegue B, Shi J, Xu X, Sorescu D, Chung AB, Griendling KK, Lambeth JD. Cell transformation by the superoxide-generating oxidase Mox1. Nature. 1999; 401:79–82. [PubMed: 10485709]
2. Alam A, Leoni G, Wentworth CC, Kwal JM, Wu H, Ardita CS, Swanson PA, Lambeth JD, Jones RM, Nusrat A, Neish AS. Redox signaling regulates commensal-mediated mucosal homeostasis and restitution and requires formyl peptide receptor 1. Mucosal immunology. 2014; 7:645–655. [PubMed: 24192910]
3. Coant N, Ben Mkaddem S, Pedruzzi E, Guichard C, Treton X, Ducroc R, Freund JN, Cazals-Hatem D, Bouhnik Y, Woerther PL, Skurnik D, Grodet A, Fay M, Biard D, Lesuffleur T, Deffert C, Moreau R, Groyer A, Krause KH, Daniel F, Ogier-Denis E. NADPH oxidase 1 modulates WNT and

NOTCH1 signaling to control the fate of proliferative progenitor cells in the colon. Molecular and cellular biology. 2010; 30:2636–2650. [PubMed: 20351171]

4. Geiszt M, Lekstrom K, Brenner S, Hewitt SM, Dana R, Malech HL, Leto TL. NAD(P)H oxidase 1, a product of differentiated colon epithelial cells, can partially replace glycoprotein 91phox in the regulated production of superoxide by phagocytes. Journal of immunology. 2003; 171:299–306.
5. Jones RM, Luo L, Ardita CS, Richardson AN, Kwon YM, Mercante JW, Alam A, Gates CL, Wu H, Swanson PA, Lambeth JD, Denning PW, Neish AS. Symbiotic lactobacilli stimulate gut epithelial proliferation via Nox-mediated generation of reactive oxygen species. The EMBO journal. 2013; 32:3017–3028. [PubMed: 24141879]
6. Leoni G, Alam A, Neumann PA, Lambeth JD, Cheng G, McCoy J, Hilgarth RS, Kundu K, Murthy N, Kusters D, Reutelingsperger C, Perretti M, Parkos CA, Neish AS, Nusrat A. Annexin A1, formyl peptide receptor, and NOX1 orchestrate epithelial repair. The Journal of clinical investigation. 2013; 123:443–454. [PubMed: 23241962]
7. Rokutan K, Kawahara T, Kuwano Y, Tominaga K, Sekiyama A, Teshima-Kondo S. NADPH oxidases in the gastrointestinal tract: a potential role of Nox1 in innate immune response and carcinogenesis. Antioxidants & redox signaling. 2006; 8:1573–1582. [PubMed: 16987012]
8. Sadok A, Bourgarel-Rey V, Gattacceca F, Penel C, Lehmann M, Kovacic H. Nox1-dependent superoxide production controls colon adenocarcinoma cell migration. Biochimica et biophysica acta. 2008; 1783:23–33. [PubMed: 18023288]
9. Ueyama T, Geiszt M, Leto TL. Involvement of Rac1 in activation of multicomponent Nox1- and Nox3-based NADPH oxidases. Molecular and cellular biology. 2006; 26:2160–2174. [PubMed: 16507994]
10. Miyano K, Ueno N, Takeya R, Sumimoto H. Direct involvement of the small GTPase Rac in activation of the superoxide-producing NADPH oxidase Nox1. The Journal of biological chemistry. 2006; 281:21857–21868. [PubMed: 16762923]
11. Cheng G, Diebold BA, Hughes Y, Lambeth JD. Nox1-dependent reactive oxygen generation is regulated by Rac1. The Journal of biological chemistry. 2006; 281:17718–17726. [PubMed: 16636067]
12. Banfi B, Clark RA, Steger K, Krause KH. Two novel proteins activate superoxide generation by the NADPH oxidase NOX1. The Journal of biological chemistry. 2003; 278:3510–3513. [PubMed: 12473664]
13. Geiszt M, Lekstrom K, Witta J, Leto TL. Proteins homologous to p47phox and p67phox support superoxide production by NAD(P)H oxidase 1 in colon epithelial cells. The Journal of biological chemistry. 2003; 278:20006–20012. [PubMed: 12657628]
14. Dutta S, Rittinger K. Regulation of NOXO1 activity through reversible interactions with p22 and NOXA1. PloS one. 2010; 5:e10478. [PubMed: 20454568]
15. Takeya R, Ueno N, Kami K, Taura M, Kohjima M, Izaki T, Nunoi H, Sumimoto H. Novel human homologues of p47phox and p67phox participate in activation of superoxide-producing NADPH oxidases. The Journal of biological chemistry. 2003; 278:25234–25246. [PubMed: 12716910]
16. Yamamoto A, Kami K, Takeya R, Sumimoto H. Interaction between the SH3 domains and C-terminal proline-rich region in NADPH oxidase organizer 1 (Noxo1). Biochemical and biophysical research communications. 2007; 352:560–565. [PubMed: 17126813]
17. Debbabi M, Kroviarski Y, Bournier O, Gougerot-Pocidalo MA, El-Benna J, Dang PM. NOXO1 phosphorylation on serine 154 is critical for optimal NADPH oxidase 1 assembly and activation. FASEB journal : official publication of the Federation of American Societies for Experimental Biology. 2013; 27:1733–1748. [PubMed: 23322165]
18. Kroviarski Y, Debbabi M, Bachoual R, Perianin A, Gougerot-Pocidalo MA, El-Benna J, Dang PM. Phosphorylation of NADPH oxidase activator 1 (NOXA1) on serine 282 by MAP kinases and on serine 172 by protein kinase C and protein kinase A prevents NOX1 hyperactivation. FASEB journal : official publication of the Federation of American Societies for Experimental Biology. 2010; 24:2077–2092. [PubMed: 20110267]
19. Kim JS, Diebold BA, Babior BM, Knaus UG, Bokoch GM. Regulation of Nox1 activity via protein kinase A-mediated phosphorylation of NoxA1 and 14-3-3 binding. The Journal of biological chemistry. 2007; 282:34787–34800. [PubMed: 17913709]

20. Streeter J, Schickling BM, Jiang S, Stanic B, Thiel WH, Gakhar L, Houtman JC, Miller FJ Jr. Phosphorylation of Nox1 regulates association with NoxA1 activation domain. Circulation research. 2014; 115:911–918. [PubMed: 25228390]
21. Yamamoto A, Takeya R, Matsumoto M, Nakayama KI, Sumimoto H. Phosphorylation of Noxo1 at threonine 341 regulates its interaction with Noxa1 and the superoxide-producing activity of Nox1. The FEBS journal. 2013; 280:5145–5159. [PubMed: 23957209]
22. Ambruso DR, Ellison MA, Thurman GW, Leto TL. Peroxiredoxin 6 translocates to the plasma membrane during neutrophil activation and is required for optimal NADPH oxidase activity. Biochimica et biophysica acta. 2012; 1823:306–315. [PubMed: 22178385]
23. Chatterjee S, Feinstein SI, Dodia C, Sorokina E, Lien YC, Nguyen S, Debolt K, Speicher D, Fisher AB. Peroxiredoxin 6 phosphorylation and subsequent phospholipase A2 activity are required for agonist-mediated activation of NADPH oxidase in mouse pulmonary microvascular endothelium and alveolar macrophages. The Journal of biological chemistry. 2011; 286:11696–11706. [PubMed: 21262967]
24. Ellison MA, Thurman GW, Ambruso DR. Phox activity of differentiated PLB-985 cells is enhanced, in an agonist specific manner, by the PLA2 activity of Prdx6-PLA2. European journal of immunology. 2012; 42:1609–1617. [PubMed: 22678913]
25. Leavey PJ, Gonzalez-Aller C, Thurman G, Kleinberg M, Rinckel L, Ambruso DW, Freeman S, Kuypers FA, Ambruso DR. A 29-kDa protein associated with p67phox expresses both peroxiredoxin and phospholipase A2 activity and enhances superoxide anion production by a cell-free system of NADPH oxidase activity. The Journal of biological chemistry. 2002; 277:45181–45187. [PubMed: 12121978]
26. Rhee SG, Woo HA, Kil IS, Bae SH. Peroxiredoxin functions as a peroxidase and a regulator and sensor of local peroxides. The Journal of biological chemistry. 2012; 287:4403–4410. [PubMed: 22147704]
27. Chen JW, Dodia C, Feinstein SI, Jain MK, Fisher AB. 1-Cys peroxiredoxin, a bifunctional enzyme with glutathione peroxidase and phospholipase A2 activities. The Journal of biological chemistry. 2000; 275:28421–28427. [PubMed: 10893423]
28. Manevich Y, Reddy KS, Shuvaeva T, Feinstein SI, Fisher AB. Structure and phospholipase function of peroxiredoxin 6: identification of the catalytic triad and its role in phospholipid substrate binding. Journal of lipid research. 2007; 48:2306–2318. [PubMed: 17652308]
29. Fisher AB, Dodia C, Manevich Y, Chen JW, Feinstein SI. Phospholipid hydroperoxides are substrates for non-selenium glutathione peroxidase. The Journal of biological chemistry. 1999; 274:21326–21334. [PubMed: 10409692]
30. Lien YC, Feinstein SI, Dodia C, Fisher AB. The roles of peroxidase and phospholipase A2 activities of peroxiredoxin 6 in protecting pulmonary microvascular endothelial cells against peroxidative stress. Antioxidants & redox signaling. 2012; 16:440–451. [PubMed: 22067043]
31. San Martin A, Griendling KK. Redox control of vascular smooth muscle migration. Antioxidants & redox signaling. 2010; 12:625–640. [PubMed: 19737088]
32. Schroder K. NADPH oxidases in redox regulation of cell adhesion and migration. Antioxidants & redox signaling. 2014; 20:2043–2058. [PubMed: 24070031]
33. Gorissen SH, Hristova M, Habibovic A, Sipsey LM, Spiess PC, Janssen-Heininger YM, van der Vliet A. Dual oxidase-1 is required for airway epithelial cell migration and bronchiolar reepithelialization after injury. American journal of respiratory cell and molecular biology. 2013; 48:337–345. [PubMed: 23239498]
34. Boudreau HE, Casterline BW, Rada B, Korzeniowska A, Leto TL. Nox4 involvement in TGF-beta and SMAD3-driven induction of the epithelial-to-mesenchymal transition and migration of breast epithelial cells. Free radical biology & medicine. 2012; 53:1489–1499. [PubMed: 22728268]
35. Bruder-Nascimento T, Chinnasamy P, Riascos-Bernal DF, Cau SB, Callera GE, Touyz RM, Tostes RC, Sibinga NE. Angiotensin II induces Fat1 expression/activation and vascular smooth muscle cell migration via Nox1-dependent reactive oxygen species generation. Journal of molecular and cellular cardiology. 2014; 66:18–26. [PubMed: 24445059]
36. Valente AJ, Yoshida T, Murthy SN, Sakamuri SS, Katsuyama M, Clark RA, Delafontaine P, Chandrasekar B. Angiotensin II enhances AT1-Nox1 binding and stimulates arterial smooth

muscle cell migration and proliferation through AT1, Nox1, and interleukin-18. American journal of physiology. Heart and circulatory physiology. 2012; 303:H282–296. [PubMed: 22636674]

37. Meng D, Lv DD, Fang J. Insulin-like growth factor-I induces reactive oxygen species production and cell migration through Nox4 and Rac1 in vascular smooth muscle cells. Cardiovascular research. 2008; 80:299–308. [PubMed: 18567639]
38. Shinohara M, Adachi Y, Mitsushita J, Kuwabara M, Nagasawa A, Harada S, Furuta S, Zhang Y, Seheli K, Miyazaki H, Kamata T. Reactive oxygen generated by NADPH oxidase 1 (Nox1) contributes to cell invasion by regulating matrix metalloprotease-9 production and cell migration. The Journal of biological chemistry. 2010; 285:4481–4488. [PubMed: 20018867]
39. Fields S, Song O. A novel genetic system to detect protein-protein interactions. Nature. 1989; 340:245–246. [PubMed: 2547163]
40. Kwon J, Shatynski KE, Chen H, Morand S, de Deken X, Miot F, Leto TL, Williams MS. The nonphagocytic NADPH oxidase Duox1 mediates a positive feedback loop during T cell receptor signaling. Science signaling. 2010; 3:ra59. [PubMed: 20682913]
41. Simpson KJ, Selfors LM, Bui J, Reynolds A, Leake D, Khvorova A, Brugge JS. Identification of genes that regulate epithelial cell migration using an siRNA screening approach. Nature cell biology. 2008; 10:1027–1038. [PubMed: 19160483]
42. Bunyak F, Palaniappan K, Nath SK, Seetharaman G. Flux Tensor Constrained Geodesic Active Contours with Sensor Fusion for Persistent Object Tracking. Journal of multimedia. 2007; 2:20–33. [PubMed: 19096530]
43. Bunyak F, Hafiane A, Palaniappan K. Histopathology tissue segmentation by combining fuzzy clustering with multiphase vector level sets. Advances in experimental medicine and biology. 2011; 696:413–424. [PubMed: 21431581]
44. Bunyak F, Palaniappan K, Chagin V, Cardoso M. Cell segmentation in time-lapse fluorescence microscopy with temporally varying sub-cellular fusion protein patterns. Conference proceedings : ... Annual International Conference of the IEEE Engineering in Medicine and Biology Society. IEEE Engineering in Medicine and Biology Society. Annual Conference. 2009; 2009:1424–1428.
45. Nath SK, Palaniappan K, Bunyak F. Cell segmentation using coupled level sets and graph-vertex coloring. Medical image computing and computer-assisted intervention : MICCAI ... International Conference on Medical Image Computing and Computer-Assisted Intervention. 2006; 9:101–108.
46. Thutupalli S, Sun M, Bunyak F, Palaniappan K, Shaevitz JW. Directional reversals enable Myxococcus xanthus cells to produce collective one-dimensional streams during fruiting-body formation. Journal of the Royal Society, Interface / the Royal Society. 2015; 12:20150049.
47. Gianni D, Bohl B, Courtneidge SA, Bokoch GM. The involvement of the tyrosine kinase c-Src in the regulation of reactive oxygen species generation mediated by NADPH oxidase-1. Molecular biology of the cell. 2008; 19:2984–2994. [PubMed: 18463161]
48. Kuwano Y, Tominaga K, Kawahara T, Sasaki H, Takeo K, Nishida K, Masuda K, Kawai T, Teshima-Kondo S, Rokutan K. Tumor necrosis factor alpha activates transcription of the NADPH oxidase organizer 1 (NOXO1) gene and upregulates superoxide production in colon epithelial cells. Free radical biology & medicine. 2008; 45:1642–1652. [PubMed: 18929641]
49. Manea A, Manea SA, Gafencu AV, Raicu M, Simionescu M. AP-1-dependent transcriptional regulation of NADPH oxidase in human aortic smooth muscle cells: role of p22phox subunit. Arteriosclerosis, thrombosis, and vascular biology. 2008; 28:878–885.
50. Chowdhury I, Mo Y, Gao L, Kazi A, Fisher AB, Feinstein SI. Oxidant stress stimulates expression of the human peroxiredoxin 6 gene by a transcriptional mechanism involving an antioxidant response element. Free radical biology & medicine. 2009; 46:146–153. [PubMed: 18973804]
51. Kuhns DB, Alvord WG, Heller T, Feld JJ, Pike KM, Marciano BE, Uzel G, DeRavin SS, Priel DA, Soule BP, Zarember KA, Malech HL, Holland SM, Gallin JI. Residual NADPH oxidase and survival in chronic granulomatous disease. The New England journal of medicine. 2010; 363:2600–2610. [PubMed: 21190454]
52. Lee I, Dodia C, Chatterjee S, Zagorski J, Mesaros C, Blair IA, Feinstein SI, Jain M, Fisher AB. A novel nontoxic inhibitor of the activation of NADPH oxidase reduces reactive oxygen species

production in mouse lung. The Journal of pharmacology and experimental therapeutics. 2013; 345:284–296. [PubMed: 23475902]

53. Lee I, Dodia C, Chatterjee S, Feinstein SI, Fisher AB. Protection against LPS-induced acute lung injury by a mechanism-based inhibitor of NADPH oxidase (type 2). American journal of physiology. Lung cellular and molecular physiology. 2014; 306:L635–644. [PubMed: 24487388]
54. Benipal B, Feinstein SI, Chatterjee S, Dodia C, Fisher AB. Inhibition of the phospholipase A2 activity of peroxiredoxin 6 prevents lung damage with exposure to hyperoxia. Redox biology. 2015; 4:321–327. [PubMed: 25637741]
55. Dana R, Leto TL, Malech HL, Levy R. Essential requirement of cytosolic phospholipase A2 for activation of the phagocyte NADPH oxidase. The Journal of biological chemistry. 1998; 273:441–445. [PubMed: 9417101]
56. Rubin BB, Downey GP, Koh A, Degousee N, Ghomashchi F, Nallan L, Stefanski E, Harkin DW, Sun C, Smart BP, Lindsay TF, Cherepanov V, Vachon E, Kelvin D, Sadilek M, Brown GE, Yaffe MB, Plumb J, Grinstein S, Glogauer M, Gelb MH. Cytosolic phospholipase A2-alpha is necessary for platelet-activating factor biosynthesis, efficient neutrophil-mediated bacterial killing, and the innate immune response to pulmonary infection: cPLA2-alpha does not regulate neutrophil NADPH oxidase activity. The Journal of biological chemistry. 2005; 280:7519–7529. [PubMed: 15475363]
57. Matono R, Miyano K, Kiyohara T, Sumimoto H. Arachidonic acid induces direct interaction of the p67(phox)-Rac complex with the phagocyte oxidase Nox2, leading to superoxide production. The Journal of biological chemistry. 2014; 289:24874–24884. [PubMed: 25056956]
58. Shiose A, Sumimoto H. Arachidonic acid and phosphorylation synergistically induce a conformational change of p47phox to activate the phagocyte NADPH oxidase. The Journal of biological chemistry. 2000; 275:13793–13801. [PubMed: 10788501]
59. de Mendez I, Adams AG, Sokolic RA, Malech HL, Leto TL. Multiple SH3 domain interactions regulate NADPH oxidase assembly in whole cells. The EMBO journal. 1996; 15:1211–1220. [PubMed: 8635453]
60. Krishnaiah SY, Dodia C, Feinstein SI, Fisher AB. p67(phox) terminates the phospholipase A(2)-derived signal for activation of NADPH oxidase (NOX2). FASEB journal : official publication of the Federation of American Societies for Experimental Biology. 2013; 27:2066–2073. [PubMed: 23401562]
61. Block K, Gorin Y, Hoover P, Williams P, Chelmicki T, Clark RA, Yoneda T, Abboud HE. NAD(P)H oxidases regulate HIF-2alpha protein expression. The Journal of biological chemistry. 2007; 282:8019–8026. [PubMed: 17200123]
62. Daugaard M, Nitsch R, Razaghi B, McDonald L, Jarrar A, Torrino S, Castillo-Lluva S, Rotblat B, Li L, Malliri A, Lemichez E, Mettouchi A, Berman JN, Penninger JM, Sorensen PH. Hace1 controls ROS generation of vertebrate Rac1-dependent NADPH oxidase complexes. Nature communications. 2013; 4:2180.
63. Shang F, Taylor A. Ubiquitin-proteasome pathway and cellular responses to oxidative stress. Free radical biology & medicine. 2011; 51:5–16. [PubMed: 21530648]
64. Kim SY, Jo HY, Kim MH, Cha YY, Choi SW, Shim JH, Kim TJ, Lee KY. H2O2-dependent hyperoxidation of peroxiredoxin 6 (Prdx6) plays a role in cellular toxicity via up-regulation of iPLA2 activity. The Journal of biological chemistry. 2008; 283:33563–33568. [PubMed: 18826942]
65. Ho JN, Lee SB, Lee SS, Yoon SH, Kang GY, Hwang SG, Um HD. Phospholipase A2 activity of peroxiredoxin 6 promotes invasion and metastasis of lung cancer cells. Molecular cancer therapeutics. 2010; 9:825–832. [PubMed: 20354123]
66. Jo M, Yun HM, Park KR, Hee Park M, Myoung Kim T, Ho Pak J, Jae Lee S, Moon DC, Park CW, Song S, Lee CK, Bae Han S, Tae Hong J. Lung tumor growth- promoting function of peroxiredoxin 6. Free radical biology & medicine. 2013; 61:453–463. [PubMed: 23643677]
67. Yun HM, Park KR, Lee HP, Lee DH, Jo M, Shin DH, Yoon DY, Han SB, Hong JT. PRDX6 promotes lung tumor progression via its GPx and iPLA2 activities. Free radical biology & medicine. 2014; 69:367–376. [PubMed: 24512906]

Highlights

- ☐ Peroxiredoxin6 (Prdx6) binds to the SH3 domain of Nox activator 1.
- ☐ Prdx6 assembles with the NADPH oxidase 1 (Nox1) complex.
- ☐ Prdx6 expression enhances Nox1-derived superoxide production.
- ☐ The Nox1-supportive effects of Prdx6 involve its phospholipase A_2 activity.
- ☐ Wild-type Prdx6 supports Nox1-mediated migration of colon epithelial cells.

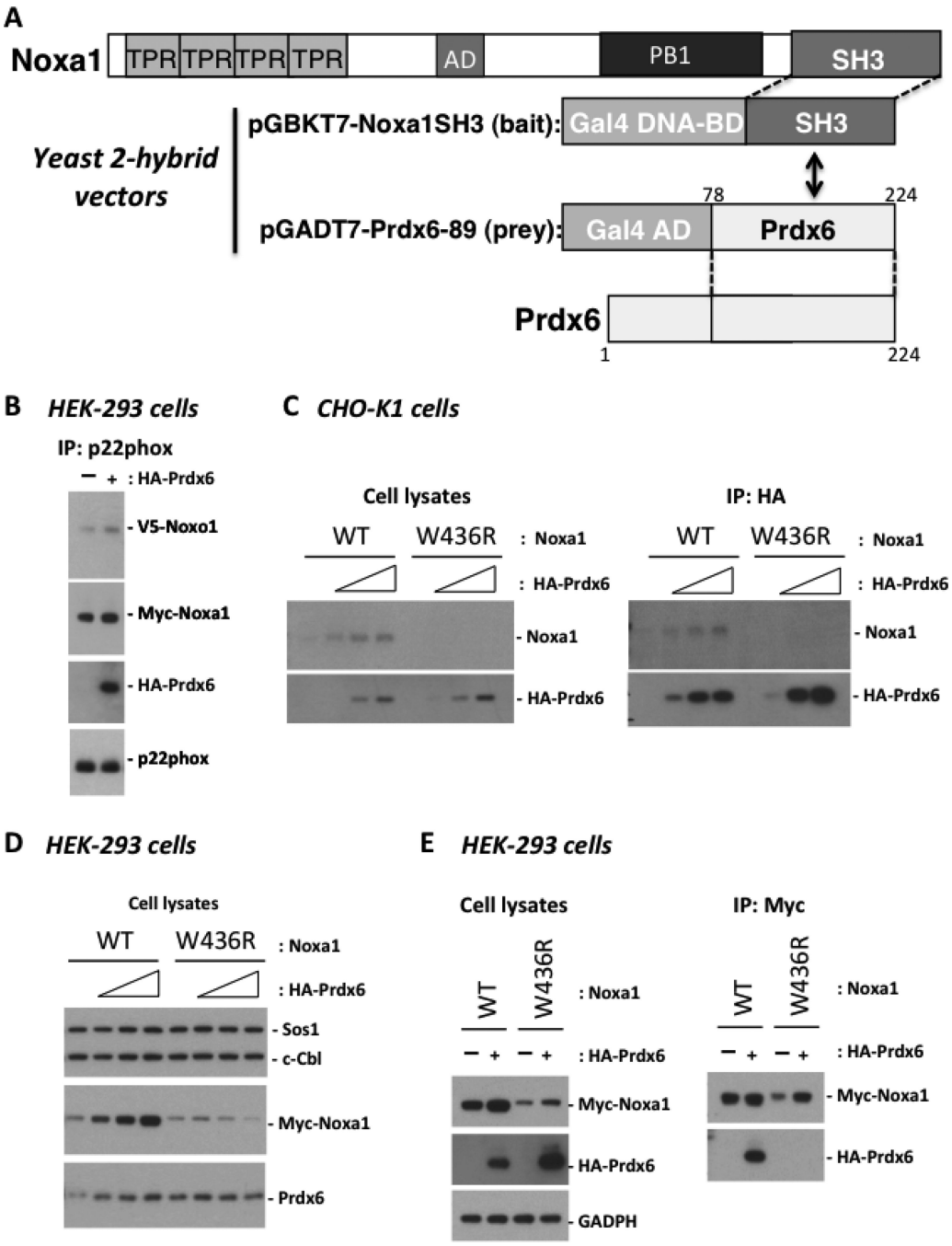

Figure 1.

Prdx6 associates with the SH3 domain of Noxa1 and stabilizes its expression. (A). Interaction of the Noxa1 C-terminal SH3 domain (res. 403-476 constructed in pGBKT7) with Prdx6 was detected by yeast two-hybrid screening of a human kidney cDNA library (expressed in pGADT7). Co-transfectants exhibited Gal4-based transcriptional activation, enabling survival on His-/Leu-/Ade-deficient selective medium. (B). Full-length Prdx6 associates with the Nox1 NADPH oxidase complex. Nox1, Noxo1, and Noxa1 encoding plasmids (0.2 ug each) were co-transfected with or without HA-Prdx6 (0.6 ug) in HEK-293

cells. Cleared cell lysates were incubated with anti-$p22^{phox}$ antibody to precipitate Nox1 complexes and associated HA-Prdx6, detected by Western blotting with anti-HA antibody. (C). Overexpressed Prdx6 enhances production of WT Noxa1 but not the SH3 domain mutant form of Noxa1 (W436R). CHO-K1 cells were co-transfected with Noxa1 plasmid (0.3 ug) and different amounts of Prdx6 plasmid (0, 0.3, 0.6, 0.9 ug) for 48 hours. Production of HA-Prdx6 and Noxa1 was analyzed in cell lysates by Western blotting with anti-HA or anti-Noxa1 antibody (left). Prdx6 associates with WT Noxa1 but not Noxa1 W436R. The cleared transfected (48hr) CHO-K1 cell lysates were harvested and incubated with anti-HA antibody to precipitate Prdx6 and associated Noxa1 (right). (D). Overexpression of HA-Prdx6 enhances detection of Noxa1 but not Noxa1 W436R in HEK-293 cells. Nox1, Noxo1, and Noxa1 (0.05 ug each) were co-transfected with HA-Prdx6 (0, 0.05, 0.1, or 0.4 ug) and the cells were processed as described in C. (E). Prdx6 associates with WT Noxa1 but not with Noxa1 W436R in HEK-293 cells. Noxa1 (0.1 ug) was co-transfected with or without Prdx6 (0.8 ug) in HEK-293 cells. Products of HA-Prdx6 and Myc-Noxa1 were analyzed in cell lysates harvested 48 hours later by Western blotting (left). Cleared lysates were also incubated with anti-Myc antibody to pull down Noxa1 and bound HA-Prdx6 detected by Western blotting (right).

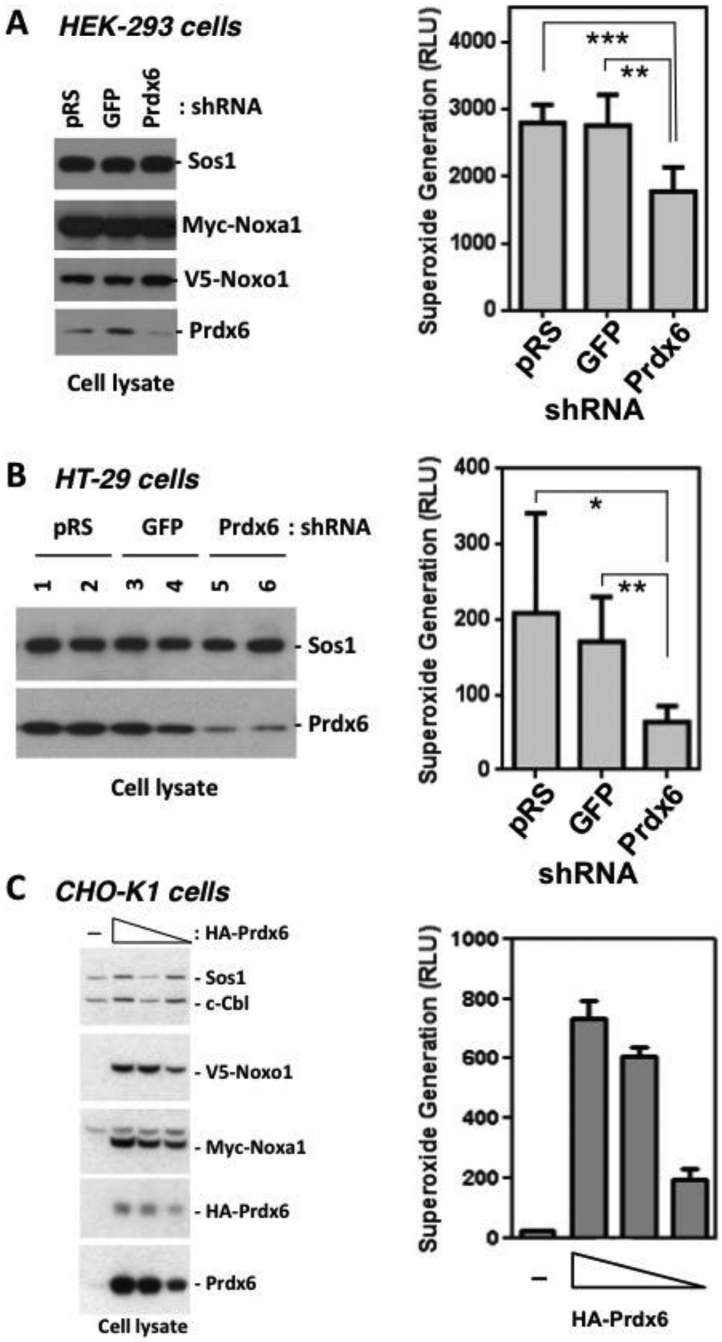

Figure 2.

Prdx6 supports Nox1 NADPH oxidase activity. (A). Transient knockdown of Prdx6 suppresses superoxide generation by Nox1 reconstituted in HEK-293 cells. Cells were co-transfected with empty vector (pRS), shRNA-GFP (GFP), or shRNA-Prdx6 (Prdx) plasmid (0.6 ug), along with Nox1, Noxo1, and Noxa1 plasmids (0.1 ug each). After 76 hours, cells were harvested for Western blotting (left) and extracellular superoxide generation (right). Unpaired *t*-test p value of Prdx6 *vs.* pRS = 0.0002. P value of Prdx6 *vs.* GFP = 0.0031. Error bars reflect mean ± S.D (n=3). (B). Stable shRNA-mediated knockdown of Prdx6 suppresses

superoxide generation by HT-29 colon epithelial cells. HT-29 cells were transfected with vector (pRS), GFP-shRNA (GFP), or Prdx6-shRNA (Prdx6) plasmids. Left panels: Western blot analysis of expressed proteins in two representative clones of each transfectant. Right: extracellular superoxide generation from trypsinized cells. Unpaired *t*-test p value of Prdx6 *vs.* pRS = 0.0245. P value of Prdx6 *vs.* GFP = 0.002. Error bars reflect mean ± S.D (n=4). (C) Overexpressed Prdx6 enhances production of transfected Nox1 components, Noxo1 and Noxa1, and extracellular superoxide generation in a dose-dependent manner. CHO-K1 cells were cotransfected (48 hrs) with various amounts of Prdx6 plasmid (0, 2, 1.5, 1 ug) along with 0.05 ug each of Nox1, Noxo1, and Noxa1 plasmids and assayed for extracellular superoxide generation (right). Left panel, cell lysates were prepared and analyzed by Western blot analysis.

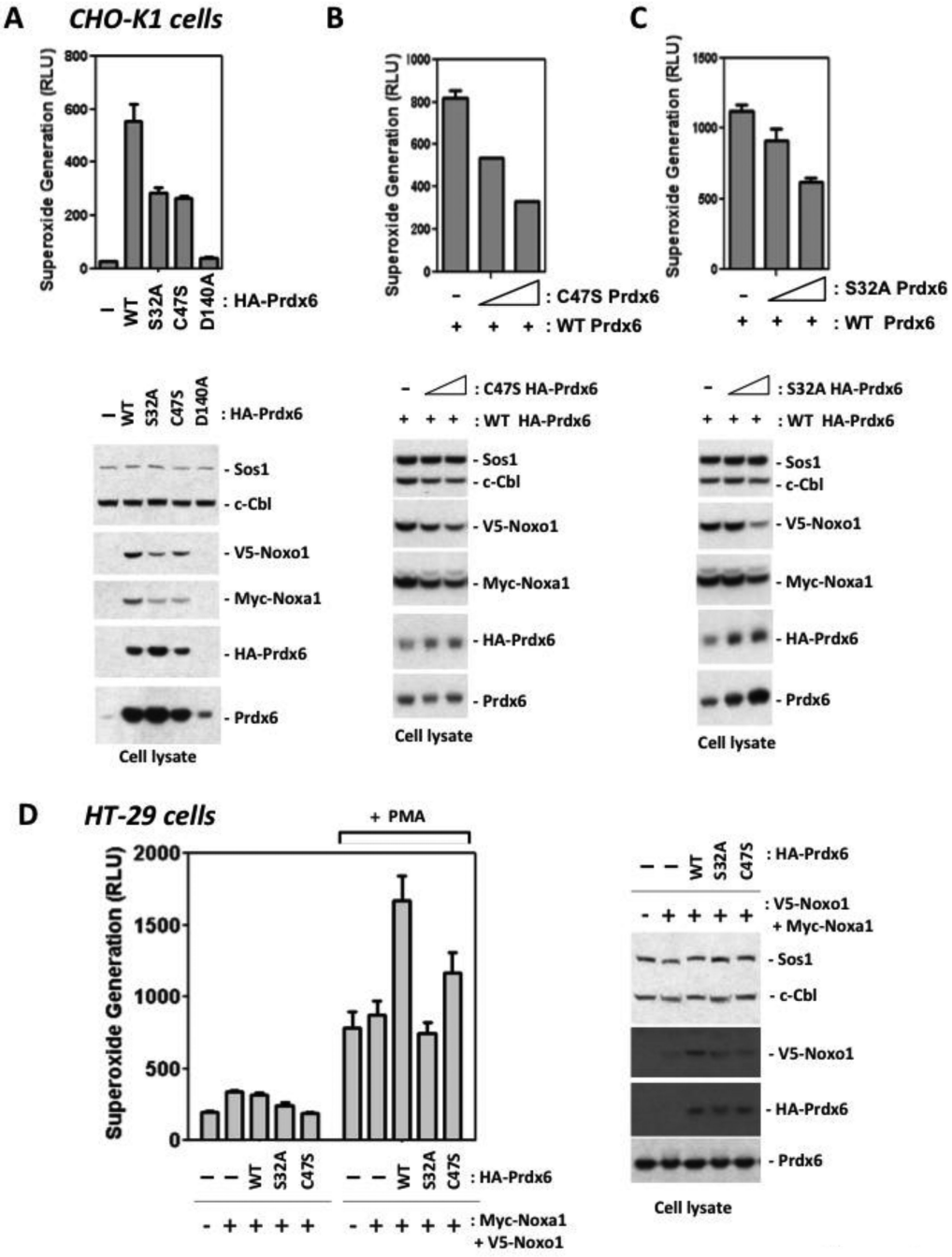

Figure 3.

Phospholipase A_2 and peroxidase mutants of Prdx6 support lower Nox1-derived superoxide generation. (A). CHO-K1 cells were co-transfected with WT, S32A (PLA_2 mutant), D140A (PLA_2 mutant), or C47S (peroxidase mutant) Prdx6 (1.5 ug), along with Nox1, Noxo1, and Noxa1 plasmids (0.05 ug each). After 48 hours, whole cell extracellular superoxide generation was measured. Cell lysates were prepared and levels of Noxo1, Noxa1, and Prdx6 were analyzed by Western blot analysis (lower panels). (B). Nox1-supportive effects of WT Prdx6 are suppressed by peroxidase mutant, C47S. Cells were co-transfected with

increasing amounts of C47S (inactive peroxidase) Prdx6 plasmid (0, 0.5, 1.5 ug), along with the same amounts of Nox1, Noxo1, Noxa1 (0.05 ug each) and WT Prdx6 (1 ug) plasmids. Upper panel: after 48 hours, extracellular superoxide generation was measured. Lower Panel: cell lysates were prepared and levels of Noxo1, Noxa1, and Prdx6 were analyzed by Western blot analysis. (C). The Nox1-supportive effects of WT Prdx6 are suppressed by PLA_2 mutant, Prdx6 S32A. Cells were co-transfected with increasing amounts of Prdx6 S32A plasmid, along with Nox1, Noxo1, Noxa1, and WT Prdx6 plasmids as in B. Upper panel: after 48 hours, extracellular superoxide generation was measured. Lower panels: cell lysates were prepared and levels of Noxo1, Noxa1, and Prdx6 were analyzed by Western blot analysis. (D). Endogenous Nox1 activity in HT-29 cells is supported by WT Prdx6 but not by Prdx6 PLA_2 or peroxidase mutants. Cells were transfected 48 hours with 2 ug of Prdx6 plasmids along with Noxo1 and Noxa1 (0.5 ug each). Left: extracellular superoxide generation in the absence or presence of PMA (1 uM) stimulation. Right: corresponding Western blotting of cell lysates. Error bars reflect mean ± S.D.; data show representative triplicate assays from one of two independent experiments.

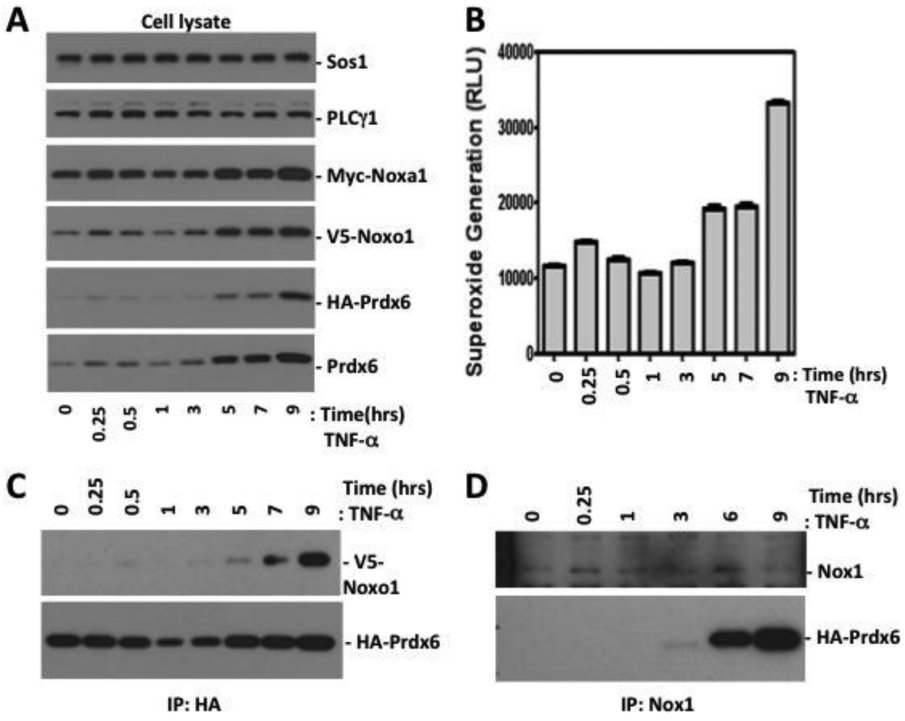

Figure 4.

TNFα induces transfected Prdx6, Noxo1, and Noxa1 levels and recruitment of Prdx6 into the Nox1 complex. (A). A stable Prdx6 knockdown clone of HEK-293 cells was co-transfected with Nox1, Noxa1, Noxo1 (0.1 ug each), and Prdx6 (0.3 ug) plasmids (48 hours) and then treated with TNFα (50 ng/ml). Cell lysates at each time point were prepared and analyzed by Western blotting. (B). Extracellular superoxide generation from trypsinized cells collected at each time point. (C). TNFα treatment induced Noxo1 recruitment into immunoprecipitated Prdx6 complexes. Lysates prepared as in A were incubated with agarose-conjugated anti-HA antibody. Co-immunoprecipitated V5-Noxo1 and HA-Prdx6 in each precipitated complex were detected with anti-V5 and anti-HA antibodies, respectively. (D) TNFα induces Prdx6 recruitment to the Nox1 immune complex at later phases. HEK-293 cells were transfected and treated with TNFα, as in B, and then cell lysates were prepared for precipitation with agarose-conjugated anti-Nox1 antibody. Prdx6 in immune complexes was detected by anti-HA Western blotting. Data show a representative blot of 2 independent experiments.

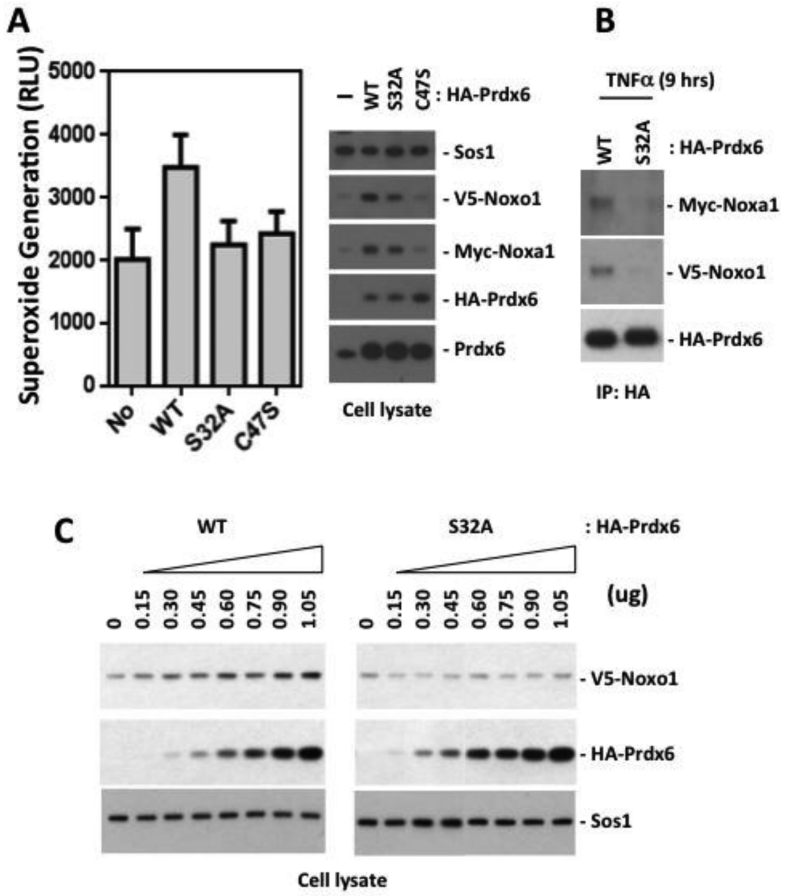

Figure 5.

PLA_2 and peroxidase mutants of Prdx6 fail to support stabilization of Nox1 components and superoxide generation in TNFα-treated HEK-293 cells. (A). Overexpressed WT Prdx6 enhanced extracellular superoxide generation in TNFα-treated HEK-293 cells, whereas PLA_2 mutant (S32A) and peroxidase mutant (C47S) forms did not. A stable Prdx6-knockdown clone of HEK-293 cells was co-transfected with or without various forms of Prdx6 (0.2 ug), along with Nox1, Noxo1, and Noxa1 (0.1 ug each). At 48 hours post-transfection, cells were treated with TNFα for 6 hours and extracellular superoxide generation from trypsinized cells was measured by the Diogenes superoxide assay. Unpaired *t*-test p value of WT Prdx6 *vs.* none (No) = 0.001. P value of WT Prdx6 *vs.* S32A = 0.0042. P value of WT Prdx6 *vs.* C47S = 0.0037. Error bars reflect mean ± S.D (n=3). Right: corresponding Western blot analysis of expressed proteins. (B). Prdx6 S32A showed a markedly reduced association with the Nox1 system in TNFα-treated HEK-293 cells. A stable Prdx6 knockdown clone of HEK-293 cells was co-transfected with Nox1, Noxa1, Noxo1, and Prdx6 plasmids WT or S32A as in A (48 hours); cells were then treated with TNFα (50 ng/ml) for 9 hours. Cell lysates were incubated with anti-HA antibody and associated Noxo1 and Noxa1 were detected with anti-V5 or anti-Myc antibody, respectively. Data show a representative blot of three independent experiments. (C). WT Prdx6 dose-dependently enhanced Noxo1 protein production, whereas Prdx6 S32A did not. HEK-293 cells were co-transfected with Nox1, Noxa1, and Noxo1 (0.1 ug each), along with increasing

amounts of Prdx6 plasmids. Cell lysates were analyzed by Western blotting with anti-V5, anti-HA, and Sos1 antibody. Data show representative blots from one of two independent experiments.

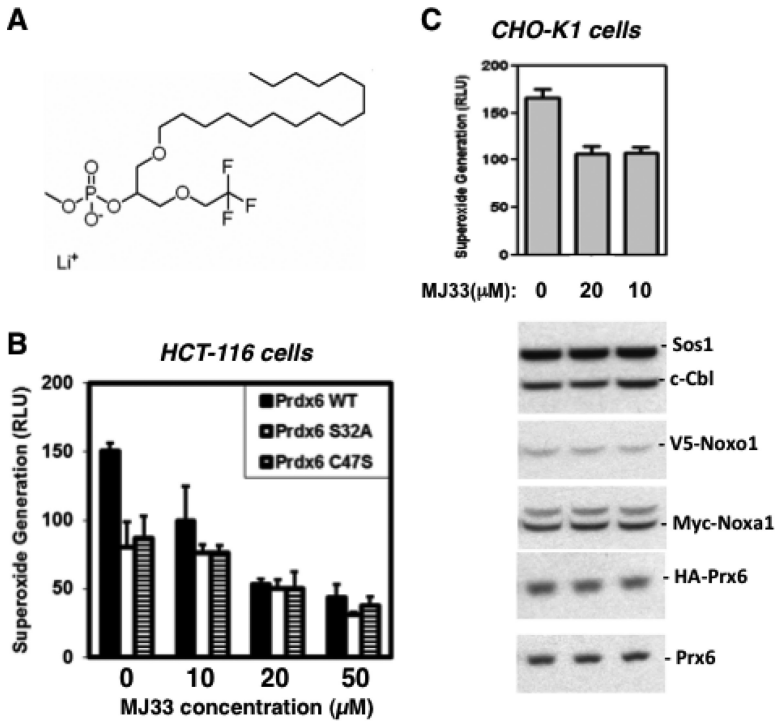

Figure 6.

Inhibition of Prdx6 phospholipase A2 activity suppresses Nox1 activity. (A) Structure of MJ33, a transition-state substrate analogue inhibitor of Prdx6 phospholipase A_2 activity. (B) MJ33 inhibits Nox1 activity reconstituted in HCT-116 cells. Cells were transfected 48 hrs with Nox1, Noxa1, Noxo1 (0.5 ug each) and WT or mutant Prdx6 (2 ug) and were then treated for 1 hr with MJ33 before harvesting for PMA-stimulated (1 uM) superoxide release assays. (C) MJ33 inhibits Nox1 reconstituted in CHO-K1 cells. Cells were transfected with Nox1, Noxo1, Noxa1 (0.05 ug) and WT Prdx6 (1 ug) for 40 hrs and then treated for 9 hrs with MJ33 before harvesting for superoxide production assays. Western blotting (lower panels) of cell lysates shows detection of Prdx6 or other Nox components was not affected by these treatments. Error bars reflect mean ± S.D (n=3). Data shown are from one of three independent experiments that gave similar results.

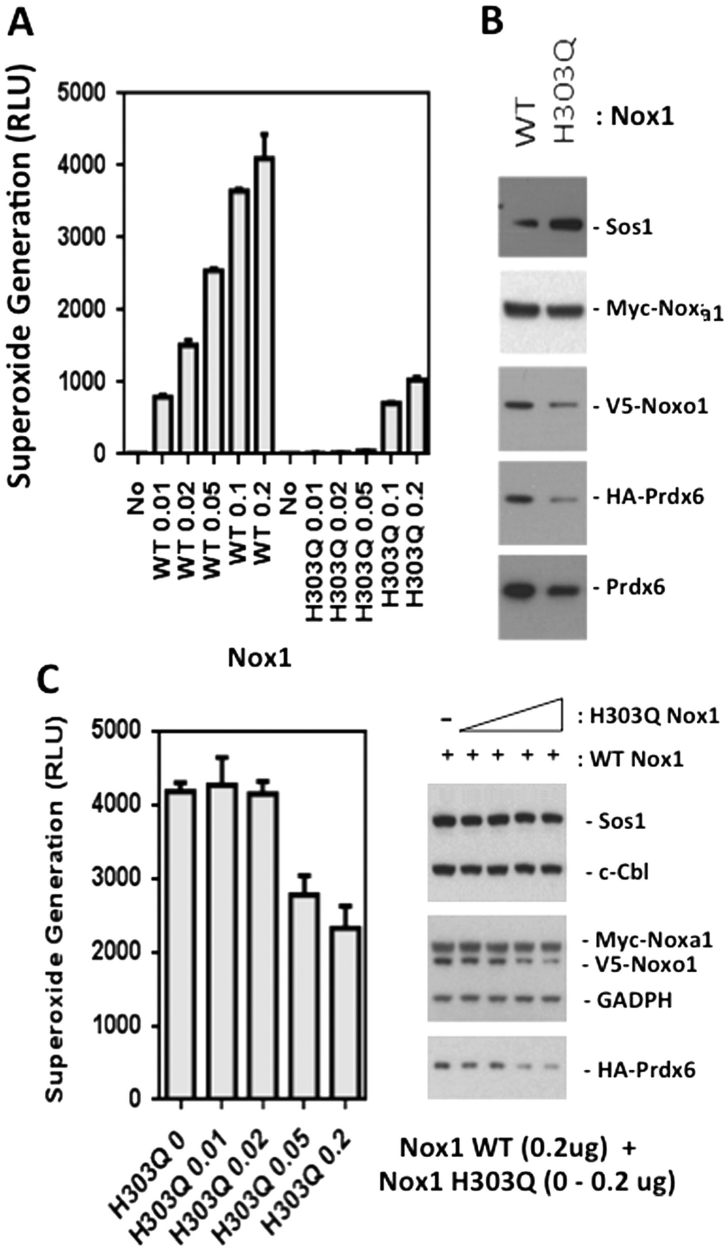

Figure 7.

Stability of the Nox1-supportive components is reduced by expression of a low activity mutant of Nox1. (A). Nox1 H303Q exhibits low superoxide generation in comparison with WT Nox1. Increasing amounts of WT or H303Q Nox1 plasmids were transfected into HEK-293 cells along with fixed amounts of Noxo1 (0.2 ug), Noxa1 (0.2 ug), and Prdx6 (0.4 ug). Trypsinized cells were assayed for extracellular superoxide generation 48 hours later. (B). Transfection of low activity Nox1 mutant (H303Q) (0.2 ug) along with Noxa1 (0.2 ug), Noxo1 (0.2 ug), and Prdx6 (0.4 ug) plasmids results in lower production of Noxa1, Noxo1, and Prdx6 in comparison with WT Nox1. (C). Co-expression of H303Q Nox1 with WT Nox1 dose-dependently suppresses detection of extracellular superoxide and Noxo1 and Prdx6 proteins. Increasing amounts of H303Q Nox1 plasmid were transfected into HEK-293

cells along with fixed amounts of Nox1 (0.2 ug), Noxo1 (0.2 ug), Noxa1 (0.2 ug), and Prdx6 (0.4 ug). Error bars reflect mean ± S.D (n=3). Right panel: corresponding Western blot analysis of proteins detected 48 hours post-transfection. Data show a representative of two independent experiments.

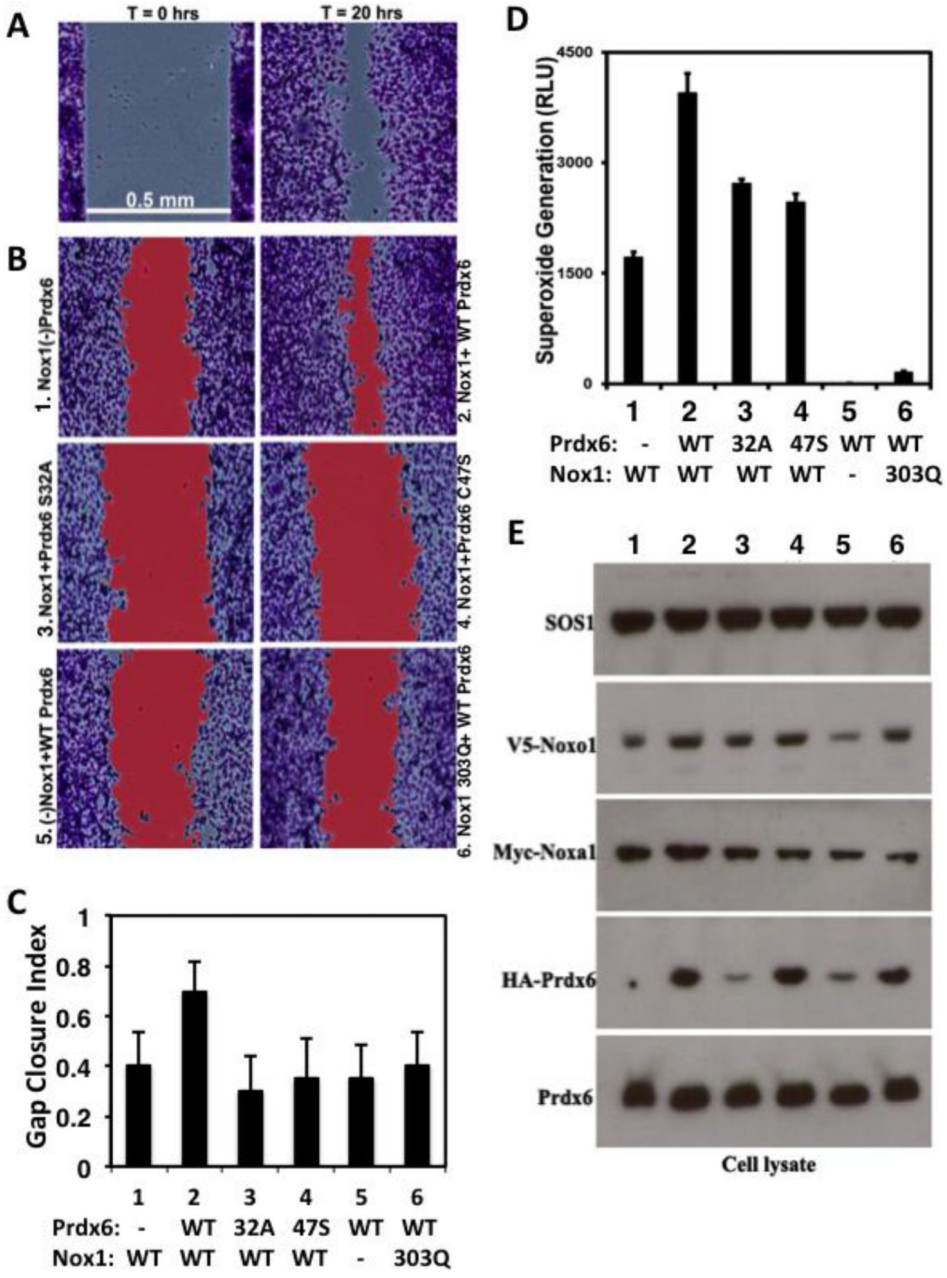

Figure 8.

Prdx6 modulates Nox1-dependent superoxide generation and migration of HCT-116 colon epithelial cells. (A). Representative fixed and stained initial (T=0, left) and endpoint (T=20 hours, right) cell migration images of HCT-116 cells transfected with Nox1, Noxo1, Noxa1, and WT Prdx6, as described in Methods. (B). Representative images after 20 hours of migration, highlighting (in red) gap areas calculated between cell boundaries, as described in Materials and Methods. All cultures (1-6) were transfected with plasmids encoding Noxo1 and Noxa1, along with various forms of Nox1, HA-Prdx6, or GFP in controls, in the absence of transfected Nox1 or Prdx6 ((−) Nox1 and (−) Prdx6, respectively). Overexpressed WT Prdx6 supports maximum Nox1-dependent colon epithelial cell migration (upper right). (C)

Mean gap closure index between migrating cell boundaries calculated at 20-hr endpoints from 3 pooled independent transfection experiments. In each experiment, 3-4 replicate Ibidi dual chambers were seeded with cells from the same series of six transfections presented in B and the endpoint gap closure index was calculated from multiple images (n= 41-54 total). Significance levels for comparisons of migration of transfection #2 (WT Nox1 and Prdx6) versus any other transfection, calculated by Welch's t-test: $p < 10^{-4}$. (D) WT Prdx6 supports enhanced PMA-stimulated Nox1-derived superoxide generation by HCT-116 cells. Shown are results of assays (48 hours post-transfection) of the same transfection series defined in C from one of three representative experiments, performed in triplicate. (E) Western blotting of HA-Prdx6 and Nox1 components from replicate transfected HCT-116 cell cultures analyzed in D. Blotting of two other transfection experiments produced similar results.

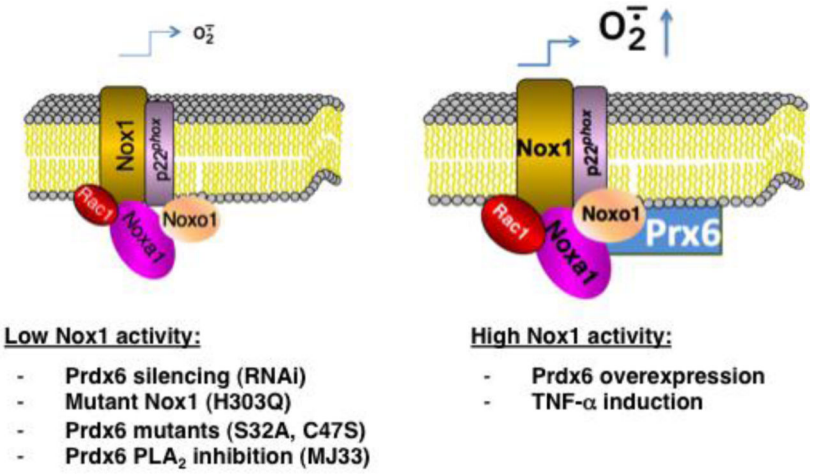

Figure 9.

Schematic summary of the Nox1-supportive effects of Prdx6. Prdx6 binds to Noxa1, assembles with the Nox1 oxidase complex, and promotes higher superoxide generation. Lower oxidase activity (left) is observed following Prdx6 silencing or expression of phospholipase or peroxidase mutant Prdx6 or mutant Nox1. The Prdx6 phospholipase A_2 inhibitor, MJ33, also suppresses Nox1 activity. TNF-α treatment or WT Prdx6 overexpression promotes higher Nox1 component production and oxidase activity (right). Nox1-derived H_2O_2 may exert positive feedback effects on oxidase activity through at least two mechanisms: inhibition of the protein degradation machinery or direct hyperoxidation of Prdx6, which may enhance its phospholipase A_2 activity [64].